REPORT NO. 556-65

INVESTIGATION AND IMPROVEMENT

OF

ZINC ELECTRODES FOR ELECTROCHEMICAL CELLS

QUARTERLY REPORT NO. 3
JANUARY 1 TO MARCH 31, 1965
Contract No. NAS 5-3873

NATIONAL AERONAUTICS AND SPACE ADMINISTRATION
GODDARD FLIGHT CENTER
GREENBELT, MARYLAND

YARDNEY ELECTRIC CORPORATION
NEW YORK, NEW YORK

Prepared by Z.O.J. Stachurski
Z.O.J. Stachurski

Approved by Dr. G.A. Dalin
Dr. G.A. Dalin

Frank Solomon, AVP

JULY 1965

TABLE OF CONTENTS

TABLE OF FIGURES

LIST OF TABLES

INTRODUCTION

In the second quarter we established that penetration of zinc through separators occurs by deposition of heavy sponge nodules within the separators. This type of sponge is formed when dendritic growth is restricted. Mossy zinc, which is the typical deposit for zinc plates which have not been overcharged and which are in early cycles, does not penetrate. We also investigated absorption isotherms of zincate in the separators and studied the density of zinc deposits as a function of zinc overpotential and other factors. In the third quarter these studies were continued.

2. Diffusion coefficient of Zincate in KOH Solutions.

To estimate the diffusion limiting current under various conditions of plating the diffusion coefficient must be known. Since no literature data are available to show how this coefficient changes in very concentrated solutions, it was necessary to measure it. Polarography on the mercury dropping electrode was used for this purpose. Pologrems were run on a Metrohm polarograph without oscillation damping. The capillary efficiency was 3.00 mg/sec and the drop times are given in the Table 2.1.

Table 2.1

KOH Concentration	Drop Time
55%	1.60 sec
25%	1.77 sec
30%	1.92 sec
35%	2.20 sec
40%	2.61 sec
44%	2.62 sec

Zinc is easily determined polarographically in certain supporting electrolytes. For example it gives a well defined wave at 1.0V in ammonia buffers (1N NH_4Cl, 1N NH_4OH)

In KOH solutions the $E_{1/2}$ is about 1.5V and if the KOH solution is concentrated the wave does not separate well from the current of the supporting electrolyte.

It was reported that for some conditions(Dirkse, Silver Migration, 2nd Quart. Rep. Aero Prop. Lab. contract Af 33(615)-1236-1964) zinc forms a double wave in concentrated KOH solutions. As is known, in concentrated electrolytes polarographic maxima of 2-nd order usually appear unless

properly damped with a surface active substance. Surface active substances damp poloragraphic maxima only in the potential range in which they are adsorbed. Most of the commonly used maxima damping substances cannot be used in concentrated KOH because of their desorption at low potentials. Consequently an apparent second wave appears above the desorption potential, which is not diffusion current but a maximum of 2-nd order.

In our 2-nd quarterly report we reported the desorption potentials of some surfactants including Triton X-100 and Igepal CO-730. The half-wave potential for zinc lies within the range of potentials in which Triton desorbs. Consequently zincate in the presence of Triton produces an apparent double wave. Igepal was shown to desrob more gradually over a much wider range of potentials which includes the zinc half-wave potential. Consequently Igepal damps the maximum completely and only a single wave appears in the zinc analysis.

Solutions of 5×10^{-3}M zincate in KOH of various concentrations were prepared, saturated with Igepal, filtered and flushed with N_2 gas for 15 minutes.

Polarograms on these solutions are shown in Fig. 1 and Fig 2. Blank polarograms without zincate are shown also.

The diffusion coefficient can be calculated from the height of the polarographic wave only if the wave represents a diffusion limited current and not a kinetically limited current. In concentrated KOH

there are at least two ways in which the zincate complex can be reduced. Transport of the electrons can be preceded by the dissociation of the zincate complex to Zn^{+2}

$$Zn(OH)_4^{-2} \rightarrow Zn^{+2} + 4OH^-$$
$$Zn^{+2} + 2e^- \rightarrow Zn^0$$

or it can be reduced directly.

$$Zn(OH)_4^{-2} + 2e \rightarrow Zn^0 + 4OH^-$$

In the case of dissociation of the complex there exists a possibility that dissociation would be a rate limiting step. The usual polarographic technique to determine whether diffusion or dissociation is limiting the overall reaction rate is to check the dependecne of the limiting current on the pressure of mercury in the mercury feed supply. Change in pressure corresponds to change in the height of the mercury level. Kinetic currents are proportional to the surface area of the drop and independent of the rate of mercury flow. Diffusion limited currents are dependent on the rate of flow and are proportional to the square root of mercury pressure (p_{Hg}).

The dependence of the polarographic limiting current of zincate (5×10^{-3}M in 35% KOH) on the square root of the mercury pressure is shown in Fig. 3. The curve is linear and the rise in height of polarographic wave indicates that the current is diffusion limited and that dissociation is not a limiting step. It does not disclose whether dissociation precedes the reduction step. If the concentration of the

complexing agent (OH^-) is increased, $E_{1/2}$ should become more negative if dissociation is involved. Otherwise $E_{1/2}$ will stay constant.

Fig. 4 shows that $E_{1/2}$ varies only by an amount corresponding to the change in Hg/HgO potential. Consequently $E_{1/2}$ is constant. The discharge of zincate ion is therefore probably limited by charge transfer of at least the first electron. We will assume for the moment that a similar mechanism is involved when plating zinc on zinc although slow surface diffusion of adatoms may be the rate limiting step in activation control.

Once it is known that the rate of zinc deposition on a mercury dropping electrode is diffusion limited the diffusion coefficient D can be calculated from the modified Ilkovic equation:

$$i_d = 607nD^{1/2} Cm^{2/3} t^{1/6} \left(1 + \frac{AD^{1/2} t^{1/6}}{m^{1/3}}\right)$$

where: i_d = the diffusion limiting current

n = the number of electrons involved in reaction = 2

C = the concentration of zincate in millimoles per liter

m = the capillary efficiency in mg/sec

t = the drop time of mercury in sec

A = constant, taken as 31.5 following Meites and Meites although some error (up to 5%) may be connected with the choice of this constant.

The height of the polarographic waves was measured in two ways - with and without correcting for current of the supporting electrolyte. Curve 1 in Fig. 5 represents the dependence of the limiting current of zincate on the concentration of KOH, measured in the normal way. It includes no correction for blanks.

Curve 2 in the same Fig. represents corrected values. Insertion of these values into the Ilkovic equation yields the diffusion coefficient as a function of KOH concentration. It is evident that for KOH concentrations up to 30% the current and therefore the diffusion coefficient stays practically constant. This works out to about $8,5 \times 10^{-6}$ cm^2/sec. At higher concentrations a sudden decrease down to 1.5×10^{-6} cm^2/sec occurs. The calculated diffusion coefficients are shwon in Fig. 6. This sudden decrease in diffusion coefficient is rather surprising. The shape of the curve does not correspond to the Einstein-Stokes equation

$$D = \frac{kT}{6\pi r\eta}$$

Where: k = Boltzmann constant — r = Particle radius

T = Absolute temperature — η = Viskosity

This equation requires that D be proportional to $\frac{1}{\eta}$.

In Fig. 7, D was plotted as $\frac{1}{\eta}$ and no linear relationship was obtained.

3. Solubility and Diffusion of Zincate in Membranes

3.1 Outline for Calculation of Zincate Solubility in Membranes.- During the zinc penetration process a growing zinc dendrite leaves the liquid phase and enters the solid phase (separator). The diffusion coefficients in the phases are obviously different. As we showed in our second quarterly report, the concentration of zincate in the two phases is also different. The diffusion coefficients and the separation coefficient of zincate between the phases then determine the concentration gradient across the membrane.

Knowledge of the zincate transport parameters is necessary for understanding of the plating of zinc inside of the separators. The determination of the diffusion coefficient is complicated by the fact that the analytical concentration of zincate in the membrane does not necessarily correspond to the concentration involved in diffusion. The difference is due to chemisorption of zincate in the membrane.

Consider now Fig. 8. Line Obcd represents the shape of the absorption curve in cellophane or PVA. It shows three distinct regions. In the first region the concentration absorbed zincate rises sharply but the slope decreases to a plateau. In the second region the slope starts to increase again. The third region is the second plateau.

That the first region represents adsorption (line Oa) is clear from the fact that the analytical concentration of zincate in the separator is many times larger than in the surrounding solution. The presence of surfactants in the solution influences the first region, probably due to competitive adsorption. This will be discussed in section 3.4.

The second region is more controversial. If the second rise represented the BET type of isotherm with formation of multilayers, then this would mean that there is practically no free zincate in the membrane.

This is incompatible with the fact that ZnO crystallizes in slightly dried membranes as will be discussed in section 3.5. It is also incompatible with the fact that zincate diffuses through membranes. Although the rate is slower than in free electrolyte nevertheless some free zincate must be involved in the process. It appears therefore that the second region corresponds to the free zincate present in the membrane (line b). The third region indicates probably that saturation of the electrolyte with zincate in the membrane occurs before the saturation of the external solution.

Let C be the total analytical concentration of zincate in the membrane. C_a = the pseudo concentration of adsorbed zinc in moles per liter of absorbed liquid adjacent to the adsorbent (organic fiber) and C_f = concentration of free zincate present in the interfibrilar liquid. Then

$$C = C_a + C_f \qquad (3.1)$$

Let C^{ou} be the zincate concentration in the external electrolyte. The experimental dependence of C on C^{ou} follows the pattern given in Fig. 8. C_f does not increase linearly with increase of the outside concentration of zincate (C^{ou}), indicating that the ratio $C_f/C^{ou} = K_p$ varies with C^{ou}.

Assume that the Nernst partition law

$$\frac{a_f}{a_{ou}} = \frac{f_f\, C_f}{f^{ou}\, C^{ou}} = K_N \qquad (3.2)$$

where the f's the activity coefficients, and the a's are the activities holds for the distribution of zincate between the membrane and the outside solution. It is further assumed that f_f/f^{ou} increases with C^{ou}.

Let us express (3.2) in terms of chemical potentials:

$$\frac{C_f}{C^{ou}} = e^{-(\Delta\mu^0 + \mu_f^E - \mu_{ou}^E)/kt} \qquad (3.3)$$

Where $\Delta\mu^0$ is the difference in standard chemical potentials between the two phases, and μ_f^E, μ_{ou}^E are the excesses of chemical potentials.

The chemical potentials(μ) are of course equal in both phases.

In (3.3) $\exp(-\mu_f^E/kT)$ represents f_f and $\exp(\mu_{ou}^E/kT)$ represents f^{ou}.

If C_s^{ou} is the outside concentration at which zincate becomes saturated in the membrane, then we can assume that when $(C^{ou} \rightarrow C_s^{ou})$ then

$\lim (\mu_f^E - \mu_{ou}^E) = \mu_1^E - \mu_2^E$ where $(\mu_1^E - \mu_2^E)$ is the difference in chemical potential excess for inner and outer zincate, when $(C^{ou} = C_s^{ou})$ and express this formally by an approximate linear relationship:

$$-(\mu_f^E - \mu_{ou}^E) \simeq -(\mu_1^E - \mu_2^E \frac{C^{ou}}{C_s^{ou}}) \qquad (3.4)$$

where μ_1^E and μ_2^E are constant.

Substituting this into Eq (3.3) gives the dependence of C_f on C^{ou}

$$C_f = C^{ou}\, K_N\, e^{-\Delta u_1^E/kt}\; e^{\Delta u_2^E/kt} \cdot C^{ou}/C_s^{ou} \qquad (3.5)$$

Let us call: $K = K_N \exp(-\Delta u_1^E/kT)$, and $K_1 = \Delta u_2^E/kT$

Then $$C_f = C^{ou} \times e^{K_1 C^{ou}/C_s^{ou}} \qquad (3.6)$$

For small values of C^{ou} when the quantity of adsorbed zincate varies, we have:

$$C_f \simeq K C_{ou} \qquad (3.7)$$

Adsorption on the fibers inside the membrane depends directly on C_f and only through C_f on C^{ou}.

Assuming that the number of adsorption sites and the heat of adsorption are constant, and utilizing Eq (3.7) we can write the Langmuir adsorption isotherm as:

$$C_s = C_\infty \frac{KK_1 C^{ou}}{1 + KK_2 C^{ou}} \qquad (3.8)$$

Where C_∞ is the limiting value of C_s, and K_2 is a constant.

Combining (3.1), (3.5), (3.6) and (3.8) we obtain an expression for the total analytical quantity of zincate in the membrane as a function of C^{ou}:

$$C = C_\infty \frac{KK_1 C^{ou}}{1 + KK_2 C^{ou}} + K\, C^{ou}\; e^{K_1 C^{ou}/C_s^{ou}} \qquad (3.9)$$

Because C_s^{ou} corresponds to the situation when C_f equals C_f^s which cannot be exceeded we supplement this isotherm by a condition

$$C_f = K C_s^{ou}\, e^{K_1} \qquad \text{for all } C^{ou} \geq C_s^{ou}$$

Note that C^{ou} can exceed C_s^{ou} if the solution supersaturates. This adsorption isotherm is important because it gives us the functional dependence of C_f and C_f/C^{ou} on C^{ou}, and especially because it permits us to calculate C_f, K, K_1, K_2, and C_s^{ou}, all of which are easily obtained. We can determine the limiting adsorption $C_s = C_\infty$ by measuring the height of the first plateau as in Fig. 8.

We can determine the adsorption coefficient K_2 from the reciprocal of the expression for Langmuir adsorption isotherm:

$$\frac{C_\infty}{C_s} = 1 + \frac{1}{KK_2} \quad \frac{1}{C^{ou}} \qquad (3.10)$$

The slope of the plot (C_∞/C_s) vs. $(C^{ou})^{-1}$, for initial part of the absorption isotherm gives us $(KK_2)^{-1}$. After determining K as given below we calculate K_2.

The constant K is found from a plot of $\ln (C_f/C^{ou})$ vs. C_s^{ou} for the value of C^{ou} in the intermediate region.

Since $$\ln C_f/C^{ou} = \ln K + K_1 C^{ou}/C_s^{ou} \qquad (3.11)$$

C_s^{ou} is read by extrapolating the curve b and plateau d to the intercept. (Fig. 8). For our purpose the range of very low C^{ou}

$$C_s + C_f = (K_2 + 1) K C^{ou} \qquad (3.12)$$

is especially important since it is in that range of C^{ou} that plating of Zn in the membranes takes place.

As will be shown later the ratio $K_p^{-1} = \frac{C^{ou}}{C_f}$ for small C^{ou} values is large. Since only free zincate can participate in the diffusion, C_f determines the rate of plating. The large value found for C^{ou}/C_f explains why separators are effective in preventing zinc penetration as long as certain conditions are fulfilled. The necessary conditions for zinc growth in the separator will be discussed later in this report.

3.2 Outline for Calculation of Zincate Distribution in the Membranes During the Stationary Diffusion.

Let us take a membrane, of thickness ℓ, between two zincate solutions I and II. Diffusion occurs along the X coordinate in the membrane. Let the interface between the membrane and solution II be at X=0, while the interface between the membrane and solution I is at X= ℓ. The concentration of zincate in solution II is equal to C^{ou}_{II}, while the concentration in solution I is C^{ou}_{I} Only the gradient of C_f across the membrane will be responsible for diffusion.

Under such conditions the flux of zincate along the X coordinate in the membrane is represented by

$$J = D_f \left(\frac{\partial C_f}{\partial X}\right) C^{ou}_{II} \qquad (3.13)$$

and will be function of C^{ou}_{II} since both D_f and C_f are functions of the outside concentration C_{ou}. C_f is dependent on C_{ou} as was shown in Eq. (3.6)

The dependence of f_f on C_f and C^{ou} is derived as follows:

Comparison of equations (3.2) and (3.5) gives

$$\frac{C_f}{C^{ou}} = K_N f^{ou}/f_f = K \exp (K_1 C^{ou}/C_s^{ou}) \qquad (3.14)$$

and $$f_f = K_N/K f^{ou} \exp (-K_1 C^{ou}/C_s^{ou}) \qquad (3.15)$$

hence $$C_f f_f = C^{ou} f^{ou} K_N \qquad (3.16)$$

Following the treatment of Onsager and Fyring we can write the diffusion coefficient as:

$$D_f = D_o'' \frac{\partial \ln N_f f_f'}{d \ln N_f} \qquad (3.17)$$

Where N_f is the mole fraction of zincate in the electrolyte present in the membrane and f_f' is the corresponding activity coefficient. Because in our case $N < 0.1$ Eq. (3.17) reduces to:

$$D_f = D_o' \frac{d \ln C_f f_f}{d \ln C_f} \qquad (3.18)$$

Substituting values for C_f and f_f in the numerator gives:

$$D_f = D_o' \frac{d \ln K_N C^{ou} f^{ou}}{d \ln C_f} \qquad (3.19)$$

Since K_N is constant and varies slowly with C^{ou}, the following approximation is valid:

$$D_f/D_o = d \ln C^{ou}/ d \ln C_f \qquad (3.20)$$

Taking the reciprocal slope of the plot of log C_f vs. log C^{ou} for a given outside concentration we can obtain the value of D_f/D_o for any C_{ou} up to saturation.

If D_o is an activity independent diffusion coefficient then the flux of zincate along the x coordinate at any moment of time at any point of the membrane is:

$$J_{x,t} = D_f\left(\frac{\partial C_f}{\partial x}\right) = D_o'\left(\frac{\partial a_f}{\partial x}\right)_{x,t} = D_o'\left(\frac{\partial C_f f_f}{\partial x}\right)_{x,t} \qquad (3.21)$$

substituting our expressions for C_f and f_f in Eq (3.21) gives

$$J_{x,t} = D_o'\left[\frac{\partial(C^{ou} f^{ou} K_N)}{\partial x}\right] = D_o\left[\frac{\partial(C^{ou} f^{ou})}{\partial x}\right] \qquad (3.22)$$

The zincate activity coefficient in concentrated KOH (f^{ou}) is probably only slightly dependent on zincate concentration but is strongly influenced by the KOH concentration.

In such a case then

$$J = D_o f^{ou} \cdot \text{Grad } C^{ou} \qquad (3.23)$$

Furthermore we can represent $D_o' = D_o K_N^{-1}$ as being equal to the diffusion coefficient of zincate in free KOH having a concentration equal to that in the membrane multiplied by some perturbation coefficient which in the simplest case will be a tortuosity coefficient Y representing the extended path of diffusion between the fibers.

The pseudo-diffusion coefficient D_p in (3.23) is given as

$$D_p = D_o f^{ou} = D'_o K_N f^{ou} = D_{NOH} Y K_N f^{ou} \qquad (3.24)$$

We call it "pseudo" because it differs from the diffusion coefficient D_f defined by Fick's first law Eq. (3.13) and (3.20).

The stationary flux from the sincate rich plane I to the sincate poor plane II is then:

$$J_{ss} = D_p (C_I^{ou} - C_{II}^{ou})/\ell \qquad (3.25)$$

Since we have expressions for C_f, C_e, D and K_p as a function of C^{ou} (at equilibrium), we can find the distribution of above values in the membrane.

From the linearity of Eq (3.25) it follows that with any distance X from plane II we can associate a concentration C_x^{ou} :

$$C_x^{ou} = C_{II}^{ou} + \left(C_I^{ou} - C_{II}^{ou}/\ell\right) . x \qquad (3.26)$$

Now if $C_{II}^{ou} = 0$, (3.26) reduces to

$$C_x^{ou} = C_I^{ou} x/\ell \qquad (3.27)$$

Inserting Eq (3.27) into Eq (3.6) and taking the logarithm of both sides gives:

$$\log C_x^f = \log K C_{II}^{ou} x/\ell + K_1 C_1^{ou} x/C_s^{ou} \ell \qquad (3.28)$$

Where C_x^f is the concentration of free sincate at any point

Having C_x^f we can calculate the concentration of adsorbed zinc (C_x^a) at any point of the membrane since from Eq (3.8)

$$C_x^a = C_\infty \left(K_2 C_x^f / [1 + K_2 C_x^f] \right) \qquad (3.29)$$

Knowing C_x^a and C_x^f we can plot the distribution of the total inner concentration of zincate C_x

$$C_x = C_x^a + C_x^f \qquad (3.30)$$

in the membrane (C_x vs. x).

3.3 Results of the calculation of zincate solubility and diffusion in cellophane from Experimental Data.

Samples of cellophane PUD-300 were soaked for 5 days in 44% KOH containing various quantities of zincate at room temperature.

After burning off the cellulose Zn was determined polarographically. The results for the dependence of the analytical content of zinc in the membrane as a function of outside concentration were analyzed in a manner described in section (3.1) to obtain the equilibrium solubility parameters.

From the plot C vs C^{ou}, the two constants, C_∞ and C_s^{ou} were determined as in Fig. 8 to be: (The number of significant figures given here do not necessarily reflect the precision of the method)

$$C_s = 0.354 \text{ moles/liter}$$
$$C_s^{ou} = 1.09 \text{ moles/liter}$$

Experimental values of C_f were found from the difference

$$C_f = C - C_\infty$$

and are given in Table 3.1.

Table 3.1

Experimental Values of C_f

C^{Cu}	C	C_f
10^{-3}	0.218	-
10^{-2}	0.296	-
10^{-1}	0.354	0
0.500	0.354	0
0.725	0.485	0.132
1.00	0.705	0.351
1.25	0.817	0.463

A plot of C_f/C^{Cu} vs. C^{Cu}/C_s^{Cu} gives the coefficients K and K_1 (cf. paragraph after Eq. 3.5). All coefficients are listed in Table 3.2.

The calculated values of C_f for various C^{Cu} are plotted in Fig. 9. Since log C_f vs. lot C^{Cu} will be necessary later in the discussion on diffusion we present it as Fig. 10. The adsorption coefficient K_2K was found from the plot C_∞/C_s vs. $(C^{Cu})^{-1}$ (cf. Eq. 3.10) by utilizing initial experimental points of C^{Cu} vs. C_f from Table 3.1. These results give K_2 as 5.59×10^4 (liter $mole^{-1}$).

The calculated absorption coefficients for zincate in cellophane are listed below.

Table 3.2

Calculated Absorption Constants for Cellophane in Zincate Solutions

$K = 3.3 \times 10^{-2}$

$K_1 = 2.44$

$K_2 = 5.59 \times 10^4$ liters $mole^{-1}$

Thus we now have the necessary data to plot the absorption isotherm Eq (3.9) and to check its agreement with the experimental results. In Fig. 11 it may be seen that the agreement is good.

The separation coefficient $K_p = C_f/C^{ou}$, is a function of C^{ou}, and this dependence is shown in Fig. 12 curve 1. For convenience of discussion also K_p^{-1} is included as curve 2.

It is evident from Fig. 12 curve 2 that when the zincate concentration outside the cellophane drops, the concentration inside drops much faster. In saturated zincate the concentration outside the membrane exceeds the concentration of free zincate in the membrane only 1½ times. This ratio changes rapidly as the solution becomes more dilute; for example in 0.01 M solution $C^{ou}/C_f = 30$.

To obtain some indication as to what is the nature of the zincate adsorption on the cellulosic fibers the ratio of moles of adsorbed zincate to number of moles of glucose in fibers was calculated. The formula for cellulose is $(C_6H_{10}O_5)_n$ with M.W. of glucose in a chain 162.14. The density of cellophane is 1.61 g/ml.

From our data the maximum quantity of adsorbed zinc (C_∞) is 0.59 moles of zincate per Kg of dry cellulose.

Therefore at maximum coverage there were 9.57×10^{-2} moles of zincate per mole of glucose. This corresponds to the adsorption of one molecule of zincate per ten molecules of glucose. This implies then that there is no adsorbtion along the cellulosic chain. The fact that one molecule of glucose can bind zincate physically or chemically and nine others cannot suggests that one molecule occupies either special

position or is in a state different from others. We can explain this assuming that zincate is adsorbed at the last molecule of a chain. We don't know how many molecules are adsorbed at such an end molecule. If n molecules are adsorbed at each end (where probably $1 \leq n \leq 4$) than mean degree of polymerization of cellophane would be $n \times 20$.

Once we have calculated C_f vs C^{ou} we can consider how the diffusion coefficient D_f changes inside the membrane as a function of concentration in the membrane. According to Eq. (3.20) the reciprocal of the slope of the plot of $\ell_n C_f$ as $\ell_n C_{ou}$ (Fig. 10) at any C_f gives us ratio D_f/D_o at this concentration. In Fig. 13, dependence of D_f/D_o on both C_f (curve 2.) and the imaginary value of C^{ou} (curve 1) is plotted.

For very dilute zincate solution $D_f = D_o$, while for concentrated solutions it falls to 10% of D_o.

Finally the distribution of total zincate content in the membrane during the stationary diffusion was calculated for various C^{ou}_{I}, when $C^{ou}_{II} = 0$.

Equations (3.28) and (3.29) were employed to calculate C^f_x and C^a_x, and their sum was plotted vs. x in Fig. 14. It is clear then that gradient of concentration is not constant.

It is only for very low outside concentrations that the concentration gradient approach linearity.

To determine the pseudo diffusion coefficient D_p in cellulosic separators, J_s was measured in a vessel composed of two compartments separated by a membrane.

One compartment of the cell was filled with 44% KOH and soaked overnight. Then zincate solution (140 MgZnO/ml) in the same concentration of KOH was added to the second compartment and increasing concentration of zincate in the first compartment was determined polarographically. D_p was calculated from Eq. (3.25) assuming that

$$C_I^{ox} \gg C_{II} \simeq 0.$$

Results are given in Table 3.3

Table 3.3

Pseudo diffusion coefficients of zinc through the cellophane separators (room temperature)

Separator	Wet Thickness (cm)	Permeation rate Moles/sec/cm^2	D_p cm^2/sec
PUD (300)	.008	1.3×10^{-8}	6×10^{-8}
C-19 (300)	.008	1×10^{-8}	4.62×10^{-8}
PUD (600)	.012	0.95×10^{-8}	8×10^{-8}
Sausage Casing (clear)	.018	0.55×10^{-8}	5.75×10^{-8}

3.4 The Influence of Surfactants on Adsorption in Separators.

In previous sections we discussed adsorption of zincate present in KOH solutions when no other substance capable of adsorption was present.

It is of interest to know whether the presence of other substances capable of adsorption influence zincate adsorption on cellophane. In this investigation samples of PUD-300 cellophane were soaked for 5 days at room temperature in the 44% KOH solutions containing increasing quanti-

ties of zincate. Three types of solution were used, Group I had no surfactant added, Group 2 was saturated with Igepal CO-730 and Group 3 was saturated with Triton X-100.

After soaking, the surface of the samples was dried by toweling. The membranes were then decomposed at 550°C and Zn determined polarographically.

The results are shown in Fig. 15. Curve 1 gives the absorption isotherm of zincate without surfactant. Curve 2 shows the influence of Igepal CO-730 on the absorption isotherm for zincate, and curve 3 shows the similar influence of Triton X-100.

It is evident that both surfactants decrease adsorption of zincate on cellophane when its concentration in the outside solution is low. In other words adsorption of surfactants on cellophane decreases number of the adsorption sites available to zincate. When the concentration of zincate is sufficiently high it displaces surfactants and in 0,5 M solutions of zincate all adsorption sites are occupied by adsorbed zincate, so that above this concentration there is no difference in C in the presence or absence of surfactants.

The increase in total zincate content in the membranes, which occurs above 0.5 M zincate, is due to increase in concentration of free zincate, and so the surfactants have no significant influence on this portion of the absorption isotherms.

3.5 Crystallisation of ZnO in Separators

Microscopic investigation of separators which were soaked in zincate solutions reveals the growth of crystals in the separators almost immediately after they are taken from the solution and towelled. This is not surprising, but it has a practical consequence. Separators in the silver-zinc cells undergo periodic wetting and drying during charge and discharge, especially since thermal effects are involved. Also, the liquid level falls in the negative compartment during discharge, exposing the tops of the separators.

Cellophane, PVA, and grafted polyethylene were examined; two distinctly different crystal sizes were observed. To determine the composition of the crystals in zincate saturated membranes several tests were performed. First a cellophane membrane was soaked for 5 days in 44% KOH containing 0.6 M zincate. Then it was taken out, blotted, inspected microscopically, boiled in water, and microphotographed (Fig. 16a). There was no distinct difference in the appearance of the membrane before and after boiling in water. In both cases large aglomerates of small crystals were observed. Next the membrane was soaked in KOH overnight at room temperature. The photograph (Fig. 16b) shows that the aglomerates disappeared. In their place a transparent apparently hollow space was left. The crystals were therefore ZnO or $Zn(OH)_2$.

Fig. 16c shows similar crystalization in PVA. What is worth noting are the cracks in the separator around the crystals. Damage to the separator is especially evident here.

Separators were soaked in solutions both with and without surfactants, and were examined microscopically. It was observed the condition of the separator was the same in both cases, although in the presence of surfactants slightly bigger crystals are formed.

3.6 Non-Stationary Diffusion of Zincate in Separators

Stationary diffusion rate studies yield what may be referred to as a pseudo-diffusion rate, D_p, as has been discussed above. To measure D_f as defined in Eq (3.13) we have to study the non-stationary stagesof diffusion. They are derived from Fick's Second Law

$$\frac{\partial C_f}{\partial t} = D_f \frac{\partial^2 C_f}{\partial x^2} \qquad (3.31)$$

Non-stationary or transient methods measure flux as a function of time. They are perhaps of even greater interest to us because sinc penetration through the seperatore is a non-stationary process.

To develop a model for the transport of sinc to the electro-crystalising tip of a dendrite one must understand better the conditions for non- stationary diffusion in the separators.

Instantaneous diffusion parameters differ considerably from those of stationary diffusion.

When the conditions for steady-state permeation are perturbed by a sudden change in concentration, there is a period immediately following the change when the diffusion flux is a function of time. This continues until new steady state conditions are established.

One non-stationary method, most frequently used for determination of diffusion coefficients, is the time lag method (Barrer, Trans. Faraday Soc., 35,628). In this method the quantity of sincate which penetrated through the membrane can be obtained at various times by integra ing the rising permeation after increasing the concentration C_I^{ou} while maintaining $C_{II}^{ou} = 0$. Extrapolation of the linear portion of the plot to J=0 gives the time lag L.

From L the value of D_f can be determined:

$$L = \frac{l^2}{6D_f} \tag{3.32}$$

DeVanathan has shown that the time lag method may be simply applied by spotting the time at which the rate of permeation is 0.6299 times the steady state value.

Another method (Devanathan, ibid.) for determining D_p utilizes the equation of a rising transient:

$$\ln\left(\frac{J - J_\infty}{J_\infty}\right)_{x=0} = \ln(1 - e^{-3t/t_o} + e^{-8\ t/t_o}) + \ln 2 - t/t_o \tag{3.33}$$

Where t_o, the rise time constant, is related to the diffusion constant by the equation:

$$t_o = \frac{\ell^2}{\pi^2 D_f} \tag{3.34}$$

A third method involves a decay time constant technique. If t equals 0 at the instant at which the permeation begins to decrease for the decay transient, it was shown that:

$$J_{(x=0)t} = J_{(x=0)t=0} e^{-t/t_o} \tag{3.35}$$

Where t_o is given by Eq (3.18). Hence a logarithmic plot of

$$\frac{J_t}{J_{(t=0)\ x=0}}$$

as a function of time should have the same gradient as the log plot for the rising transient as D is the same.

A typical permeation transient is shown in Fig. 17. This is a plot of diffusion flux J vs time. Curve (1) corresponds to the case when adsorption does not influence the transient.

Permeation into a membrane starts at t=0 due to a sudden increase in C^{ou}_{I} while C^{ou}_{II} is constant. For a certain period of time there is no response. Then the permeation starts and increases rapidly until the plateau of steady permeation is reached. Decay transient starts when C^{ou}_{I} is decreased back to C^{ou}_{II}. The time lag for this curve is

indicated by L. The term J_∞ represents the steady-state permeation flux.

Curve 2 in the same figure shows the influence of adsorption on the permeation transient. The time lag L_a is extended here. The quantity of the adsorbed zincate can be calculated from the difference between the integrals of curves (1) and (2).

In order to measure the permeation transients an apparatus shown in Fig. 18 was devised. The test membrane (1) is fixed with epoxy resin to lucite tubing, and covered a layer of mercury (2). The mercury was connected by means of a sliding contact to a potentiostat. The mercury was polarized cathodically against the counter electrode (3) and its potential is maintained constant with respect to the reference electrode (4) by means of the potentiostat (5). The cathode with the membrane is rotated by a motor (6) regulated by an electronic speed regulator(7). The cell is initially filled with KOH solution deaerated by flushing with N_2. To start the diffusion transient zincate solution is injected by a syringe (10). Zincate diffuses through the membrane and when it reaches the cathode current starts to flow. The concentration of zincate on the inner side of the membrane is maintained at zero because any zincate reaching the cathode is reduced immediately to zinc metal. Controlled rotation was necessary to eliminate formation of the boundary layer and maintain a constant and known concentration at the surface of the membrane. Therefore, the conditions necessary to measure the transient are fulfilled.

After the steady flux is reached the decay transient can be made by displacing the zincate solution in the main cell by KOH from vessel (8). Flow of the liquid from the cell is through an outlet not indicated in the figure. Preliminary experiments were run with this set up. Data will be presented in the final report.

4. Zinc Plating

4.1 Polarization of Shape Changed Zinc Electrodes

Zinc penetration through seperators seems to be correlated to zinc shape change. Shape change can be characterised by three elements: 1. rate of decrease in geometric area of plated zinc with number of cycles ($-dA_n^g/dn$); 2. rate of decrease in real surface area per unit of geometrical area of still active zinc ($A_r/A^g = A^o$ = roughness factor) with number of cycles (n) ($-dA^o/dn$); 3. rate of change in density of zinc deposit.

In view of our previous experiments with a tunnel cell we know that density of the zinc deposit is a function of zinc overpotential. We know also that change in density leads to a change from the mossy to the dendritic type of deposit. During the galvanostatic charging the zinc overpotential is a function of the real surface area of active zinc (A_r) . A_r changes with the number of cycles as:

$$\left(\frac{dA_r}{dn}\right)_n = A_o \left(\frac{dA^g}{dn}\right)_n + A^g \left(\frac{dA^o}{dn}\right)_n \qquad (4.1)$$

There is a positive feedback between the second term of the right side of 4.1 and the density. Decrease of A^g with n leads to increase of current density, which causes increase in the overpotential. Increase in overpotential causes increase in zinc density, and decrease in A^o. Consequently the process of increasing density of the zinc is self-accelerating.

In an experiment described below the rise in charging overpotential was used as an indicator of the above effect.

Two zinc oxide electrodes (1 29/32 x 3 1/8 = 5.96 in^2 containing 8 gm of a mixture of zinc oxide with 3.3% teflon and 2% HgO on 4/0 Exmet grid) were used in the experiment. One of the electrodes had been cycled for 68 cycles in a Silver-Zinc cell. The charging current was 42 ma/in^2, discharge current was 60 ma/in^2. The other electrode served as a control. Both electrodes were charged in a dummy cells connected in series, to a half of the theoretical capacity. Polarization curves were run and the results are shown in Fig. 19. Decrease in A^E on the cycled plate was about 50%. Zinc shape change on the cycled plate is shown in the lower right corner of the figure. Decrease in current was much more the 2I, which suggests that A^o was decreased.

4.2 Electroplating of Zinc on the Rotating Disc Electrode

Whether zinc is plated from the free zincate solution on a stationary electrode or on a rotated electrode, after a certain time the diffusion layer reaches a constant thickness. On a stationary electrode natural convection is responsible. Control of natural convection during the plating is a rather cumbersome task. Thermal effects accompany plating itself. The electrolyte changes density. Even the shape and size of the cell can have some influence on the process. This gives rise to poor reproducibility of the results. Replacing the natural convection by a forced flow improves the control of the plating process without essentially changing the mechanism. Parameters related to energy of activation will be the same in both cases. The only real difference is in the thickness of the diffusion layer, and rotation

permits us to vary that in accordance with the requirements of our experiments. This is the reason why we did study plating on a rotating disc electrode in our program.

The set up used in our experiments on plating on the rotating disc electrode was described in the first quarterly report. All experiments were run at room temperature and in 35% KOH. Zinc plating was run on silver discs.

We will consider first plating from the saturated zincate. To determine the value of the diffusion limited current a voltamperometric curve was measured(Fig. 20, curve 1). A plateau of diffusion limited current is well formed, and corresponds to about 700 mA/in^2 (109 mA/cm^2). The half wave potential was 120 mV vs. a zinc reference electrode in saturated zincate. Below this potential the plating is predominantly activation controlled, while at higher potentials it is predominantly diffusion controlled.

Theoretically, the half wave should be independent on the speed of rotation as well as concentration of zincate. It is important that there is very little "hysterisis" if the measurement is repeated fast increasing and then decreasing the negative potential curve 2 in Fig. 20 shows the current values after a quantity of zinc equivalent to 94 coulombs was plated. There is practically no difference in the half wave potential before and after plating. The limiting current is slightly higher after plating. Plotting a Tafel line from Fig. 20 an exchange current (i_o) of zinc was found to be 0.008A/cm^2, for roughness factor 2.

Changes of current with time during the potentiostatic plating are shown in Fig. 21. The end point of each curve corresponds to 188 coulombs of plating. After the initial rise the current value becomes almost constant for all overpotentials between 20 and 220 mV.

Similar experiments were performed for lower concentrations of zincate. The half wave potential was constant for zincate concentrations between 1M and 5×10^{-3}M (Fig. 22).

The potentiostatic plating from the dilute solutions (Fig. 23) shows an increase of plating current with time.

In order to check if the formulas derived for the calculation of the thickness of the diffusion layer (δ) for rotating disc electrodes can be applied to the case where a rough deposit has formed on the surface of the electrode, the Levich equation for thickness of the diffusion layer with laminar flow was used:

$$\delta = 1.6 \cdot D^{1/3} \gamma^{1/6} \omega^{-1/2}$$

Where D = the diffusion coefficient of zincate in KOH = $3 \times 10^{-6} cm^2 sec^{-1}$ in 35% KOH (cf. Sec 2)

γ = kinematic viscosity = $\frac{\text{viscosity}}{\text{density}} = 2.281 \times 10^{-2}$ Stokes

ω = angular rotation speed (radians/sec)

Reynold's numbers ($Re = \frac{r^2}{\delta}$) were calculated. They were much smaller than those for which turbulent flow starts, which are between 2500 and 3500. In the above equation, r is the disc radius.

The diffusion limited current is given approximately by the equation:

$$i_d = \frac{nFDC}{\delta}$$

Where i_d = the diffusion limited current

n = the number of electrons = 2

F = the faraday = 96,500 coulombs

C = the concentration of zincate in moles/cm^3

Calculated and experimental values for the limiting current at the beginning and the end of plating of 94 coulombs as a function of the square root of the rotation speed are shown in Fig. 24. The agreement between the calculated i_d for laminar flow and the experimental values obtained at the beginning of the plating is good as can be seen in Fig. 24 and 25. After the plating deviation from the linear dependence is more considerable. Microscopic inspection of the discs after plating at the half wave potential (95 mV) and at the value obtained for the diffusion limited current(220 mV) showed a dendritic deposit. The increase was therefore probably due to some contribution of turbulence around the electrode. Flow nevertheless cannot be considered as completely turbulent because the experimental values of i_d after plating are much closer to the theoretical i_d calculated for laminar flow than to the i_d calculated for turbulent flow.

δ for turbulent flow was calculated from the Vielstich equation:

$$\delta = r\left(\frac{r^2\omega}{\gamma}\right)^{-0.9}\left(\frac{\gamma}{D}\right)^{-1/3}$$

A comparison of experimental data with those calculated for laminar and turbulent flow is given in Table 4.1

TABLE 4.1

Conc. Zincate (moles)/cc	ω Rad/Sec	Re	δ Lam cm	δ Turb cm	Theoretical i_d Lam mA/cm^2	Theoretical i_d Turb mA.cm^2	i_d Exp Before	i_d Exp After
10^{-5}	97.9	1330	1.25×10^{-5}	4.38×10^{-5}	4.66	132.1	5.54	
7.6×10^{-6}	97.9	1330	1.25×10^{-3}	4.38×10^{-5}	3.54	100.3	4.23	7.09
5.4×10^{-6}	97.9	1330	1.25×10^{-3}	4.38×10^{-5}	2.52	71.3		
10^{-5}	55.1	748	1.66×10^{-3}		3.48		3.46	
7.6×10^{-6}	55.1	748	1.66×10^{-3}		2.64		2.64	4.26
5.4×10^{-6}	55.1	748	1.66×10^{-3}		1.88			
10^{-5}	21.3	290	2.65×10^{-3}	1.81×10^{-4}	2.16	31.95	2.58	
7.6×10^{-6}	21.3	290	2.68×10^{-3}	1.81×10^{-4}	1.64	24.25	2.03	2.29
5.4×10^{-6}	21.3	290	2.68×10^{-3}	1.81×10^{-4}	1.15	17.25	1.35	

5. Model of Zinc Plating

5.1 Zinc Plating from the Solutions

Any model of zinc plating should explain at least qualitatively why 3 types of zinc deposits are possible: smooth, mossy and dendritic, and their dependence on the overpotential (η), C and ω. More specifically, the following facts should be explained:

1. Why smooth deposits are formed only at high rotation speeds (when Re is close to or exceeds 2500), at low overpotentials ($<$-50 mV) in concentrated zincate solutions (0.1 - 1.3 M).

2. Why mossy deposits form under the following conditions:

   η low (0-100 mV)

   Re low ($<$ 1000)

   C high (0.1 - 1.3 M)

   The following properties characterize mossy deposits: Almost constant diameter (0.6 - 1.0 μ); the density of the mossy deposit increases with η and with ω, and is independent of the thickness of the plated layer but increases greatly due to adsorption of certain surfactants. Whiskers form on plating in a ZnO slurry.

3. Why dendritic deposits form at high η ($>$100 mV) and preferably at low C. Dendrites are characterised by variable diameter, branching, and changes of density with thickness of plated layer. Dendrites are not formed when plating in a ZnO slurry.

In order to explain above facts qualitatively, we suggest a physical model which can serve at least as a preliminary working hypothesis.

Consider first the beginning of the plating. Two possibilities exist. Either the type of the deposit depends on the nature of the current collector on which we plate, or it does not. Experiments of plating on sheets of zinc, cadmium, silver, stainless steel, steel,

and copper show that after a short initial period there are no differences between the type of deposits. It is possible to obtain smooth, mossy, and dendritic deposits on any of the above metals. We assume therefore the following: the surface of any of the above metals apparently has much larger number of active centers on which nucleation of zinc will take place than the number of whiskers or dendrites which eventually will form on it. The nature of these centers seems to be irrelevant.

Smooth plating occurs at high Reynold's numbers for which diffusion limiting currents are very high, and at low overpotentials. In other words, smooth plating takes place under the conditions of exclusive activation control. Plating apparently takes place both at points of high and low surface energy.

When Re is low the situation seems to be different, and the deposit becomes simultaneously activation and diffusion controlled. Let us assume then that the plating starts at various centers with an uneven rate. The real initial current density in active spots must be high, and must be low elsewhere. When there is not enough flow, local diffusion layers of thickness δ are formed around the active spots so that $(dx_\delta/dt)_{y,z} > 0$, where $X_\delta = \delta + (X)$, $(-X)$ being the distance between the current collector and the diffusion layer; and (y,z) is the plane of the electrode. There are two possibilities. Either the deposit in an active spot fulfils the condition:

$$dl/dt = dX_\delta/dt \qquad (5.1)$$

and follows the expanding diffusion layer, and whisker forms; or $dl/dt < dX_d/dt$, and the whisker, although begun, stays behind the front of those whiskers which have the necessary rate of growth. In such a case it becomes concentration polarised and stops growing. The growing whiskers which fulfil condition(5.1) form the mossy deposit.

The situation accompanying the steady growth of a mossy deposit is diagrammatically shown in Fig. 26. Consider whiskers A and B, We can distinguish three regions on each whisker: (1) The tip, which has an easy access to the free electrolyte and therefore at low overpotentials plating on it is entirely charge transfer controlled; (2) The intermediate region, in which there is a contribution of concentration (diffusion) overpotential, η_d. The total overpotential is then $\eta = \eta_a + \eta_d$ (cf. Fig. 26). Where η_a is charge transfer overpotential. This is because the concentration of zincate inside of the foam becomes more and more depleted (Fig. 26); (3) The third region in which whiskers are completely polarised due to consumption of available zincate, before it reaches this region. We have here $\eta = \eta_d$. This model therefore shows how the deposit can be activation and diffusion controlled at the same time. Plating takes place in both regions (1) and (2) up to the depth $\delta' + \delta$ in the deposit, where δ' is the thickness of the activation controlled region on the growing zinc deposit and δ the thickness of the mixed activation and diffusion controlled region. Consequently the rate of plating (I = current) is as follows:

$I = nF(dm/dt) = nF(dm_{\delta}'/dt + dm_{\delta}/dt = I_{\delta}' + I_{\delta} = I_{\delta} + I_d$

Where m is amount plated (in moles)

dm_{δ}'/dt is the rate of plating on the tip under the exclusive charge transfer control

dm_{δ}/dt is the rate of side plating in δ .

Let two whiskers B and C start growing toward each other (Fig. 26a). Then we will have:

$$(\eta - \eta_d)_I < (\eta - \eta_d)_{II} \qquad (5.2)$$

$$\eta_{aI} < \eta_{aII} \qquad (5.3)$$

Where η_{aI} is the activation overpotential on the side of whisker C adjacent to whisker B and

η_{aII} is the activation overpotential on the side of whisker C remote from whisker B

due to mutual screening of the diffusion flux, so

$$I_{\delta}^{I} < I_{\delta}^{II} \qquad (5.4)$$

Consequently the whiskesrs B and C will change their direction away from each other. Whiskers therefore grow so to avoid each other. As a result of frequent changes in the direction of growth of every whisker, a complicated network is found as indicated by our micro-photographs. This explains how the number of whiskers per unit geometrical area of cross section stays constant during the plating.

In order to get some idea of how δ and d (2d being the distance between the center of the tips of adjacent whiskers) are related to η, a simplified calculation of their interdependence was made.

Simplification is due mainly to linearization of all exponential functions involved.

The assumptions are as follows:

1. The total current (I) on a single whisker is

$$I = I_a + I_d \tag{5.5}$$

where I_a is the diffusion independent plating current and

I_d is the diffusion dependent current

2. For $\delta' << \delta$ $\quad I \simeq I_d$ (5.6)

3. The diffusion flux vector of zincate, (J) has a non zero value only in the diffusion region (2) of width δ.

4. Plating is stationary ($d\delta/dt = 0$) along the whisker growing in the x direction.

5. All J vectors subtend the same solid angle tan d/δ with the x axis and are directed towards it. (cf vectors Fig. 26)

Consequently:

$$d = \lim_{(\delta - x) \to \delta} r \tag{5.7}$$

The following relationship hold

$$d^2 + \delta^2 = \lambda_d^2 \tag{5.8}$$

$$\frac{\lambda_r}{\lambda} = \frac{x}{d} \tag{5.9}$$

$$\delta - x = \frac{\delta r}{d} \tag{.10}$$

r - cannot exceed d without interfering with the flux of the neighboring whiskers.

6. The concentration overpotential gradient in the layer is:

$$-\frac{d\eta_d}{d(\delta-x)} = -\frac{\eta}{\delta} \tag{5.11}$$

hence: $$d\eta_d = \frac{\eta}{\delta}\, d(\delta-x) \tag{5.12}$$

and: $$\eta_d = \frac{\eta}{\delta}(\delta-x) \tag{5.13}$$

7. The surface concentration C_s at any point along the whisker is:

$$C_s = C^{ou}(1 - \eta_d/\eta) \tag{5.14}$$

and from assumption (6)

$$C_s = C^{ou}\left(1 - \frac{\delta - x}{\delta}\right) \tag{5.15}$$

8. In the linear approximation:

$$I = S\, i_o\, nF/RT\, (\eta - \eta_d) \tag{5.16}$$

where S is the plating surface area and i_o the exchange current density.

9. If a whisker is considered as an elongated cylinder

$$S_w = 2\pi\rho\delta \tag{5.17}$$

where S_w is the surface area of the whisker and between x=0 and $x=\delta$, ρ is the radius of the whisker.

10. Considering the $d \gg \rho$ we neglect S_w while calculating the diffusion flux to it, but we take S_w into account to calculate the plating current.

We calculate first a diffusion flux J. This is the flux from the current source of zincate of area $S = \pi d^2$, placed at the tip of a one dimensional whisker, to the end portion δ of this whisker.

The flux through the surface element dS along λ_r is equal to:

$$dJ = D\,(dC/dy_r)_{y_r} \quad dS'_{\lambda_r, Y} \tag{5.18}$$

where Y_r is a point on λ_r, and

$dS'_{\lambda_r y}$ is a surface element normal to λ_r at y.

$dS'_{\lambda_r, Y}$ decreases when $Y/\lambda_r \to 0$.

$$dS'_{\lambda_r, y} = dS'_{\lambda_r} \quad y/\lambda_r \tag{5.19}$$

where dS'_{λ_r} is a surface element on λ_r at $y = \lambda_r$

Grad C increases when $y/\lambda_r \to 0$

$$(dC/dy)_y = (dC/dy)_{\lambda_r} \quad \frac{y}{\lambda_r} \tag{5.20}$$

The flux therefore is:

$$dJ = D\,(dC/dy)_{\lambda_r}\,dS' \qquad (5.21)$$

We can therefore treat the problem as if grad C was a constant and write:

$$dJ = D\left[(C^{ou} - C_s)/\lambda_r\right] dS' \qquad (5.22)$$

$$dS' = r\,d\phi\,dr' = r d\phi\,\frac{\delta}{\lambda}\,dr \qquad (5.23)$$

where ϕ is the radial angle along the whisker in the y,z plane, where dr' is the height of dS' which is normal to λ_r, and dr is the height of dS' which lies in the plane normal to x .

Since $\lambda_r = r/d\,\lambda_d$ (5.24)

and

$$C_s = C^{ou}\,(1 - (\delta - x)/\delta) \qquad (5.25)$$

then $$dJ = D\left[(C^{ou}\,d(\delta - x))/\lambda^2\right] .\, d\phi\,dr \qquad (5.26)$$

but $\delta - x = \delta r/d$

so $$dJ = D\,C^{ou}\,\delta\,r/\lambda^2\,.\,d\phi\,dr \qquad (5.27)$$

Intergrating equation (5.27) from 0 to 2π and 0 to d and substitution of the value of λ yields:

$$J = D\,C^{ou}\left[\delta\,d^2/(\delta^2 + d^2)\right]\pi \qquad (5.28)$$

Therefore, the current resulting from the flux is:

$$I = nF\, DC^{ou}\, \pi \left[\delta d^2 / (\delta^2 + d^2) \right] \qquad (5.29)$$

We shall calculate now the current of plating as a function of η. Substituting (5.17) and (5.13) into (5.14), and considering the resulting current only over the element of surface area $2\pi\rho\, d(\delta - x)$, gives:

$$dI = 2\pi\rho\, d(\delta - x)\; i_o (nF/RT) \cdot \eta / \delta \cdot d(\delta - x) \qquad (5.30)$$

Substituting $d(\delta - x) = (\delta/d)\, dr$, and integrating we obtain

$$I = 2\pi\rho\, i_o (nF/RT)\, \delta\, n/d^2 \int_0^{\pi} \int_0^{d} d^2\, r\, d\varphi \qquad (5.31)$$

$$I = 2\pi^2 \rho \delta i_o\, (nF/RT) \cdot \eta \qquad (5.32)$$

Substituting:

$$i_o = nF\, C^{ou}\, k \qquad (5.33)$$

where k is a mate constant (cm/sec), and compering with (5.29) gives:

$$d^2/(\delta^2 + d^2) = 2\pi/D \cdot (nF/RT) \rho k \eta \qquad (5.34)$$

or:

$$\frac{\delta}{d} = \sqrt{\frac{RT}{2\pi nF} \frac{D}{\rho k \eta} - 1} \qquad (5.35)$$

This equation is valid only when:

$$RTD/2\pi nF\rho km > 1 \qquad (5.36)$$

We shall calculate δ/d in 35% KOH saturated with zincate as a function of η . The range of η was chosen as 0 to 150 mV. This is the range in which the approximations taken are valid. The parameters are as follows:

$n = 2$

$RT/F = 26 \times 10^{-3}$ volts

$D = 5 \times 10^{-6}$ cm^2/sec

$k = 4.16 \times 10^{-5}$ cm/sec

$\rho = 4 \times 10^{-5}$ cm

A plot of δ/d vs η is shown in Fig. 27. We know that the distance between the dendrites decreases with η . Therefore, Fig. 27 shows that δ decreases rapidly with η at low overpotentials (below 100 mV). Above 100 mV changes are slow. The thickness of the inner diffusion layer δ is determined by d, D, k, and η . When sufficiently high overpotential is applied to the whisker the outer diffusion layer will start forming while the inner will vanish. The difference between the two is that the inner diffusion layer was following the growing tip of the whisker, while the outer diffusion layer precedes it. The change from the mossy deposit to dendritic is probably related to this change.

Such a situation in which the outer diffusion layer is formed is shown in Fig. 26b. No steady state will exist in this case. This means that between two instants of time t_1 and t_2, δ will increase from δ_{t_1} to δ_{t_2} (Fig. 26c).

The condition of mossy plating $dX_\delta/dt = dl/dt$ is not fulfilled and instead we have the inequality $dX_\delta/dt > dl/dt$. This means that the front of the diffusion moves faster than the increase in length of the dendrite.

The problem of constancy of radius (ρ) of whiskers can be best explained on the basis of the theory of Barton and Bockris. It shows how the activation overpotential changes with the radius of curviture of a dendrite at the tip, which can prevent ρ from further growth. (Proc. Roy Soc., 268, (1962) p.485.) This will be discussed in the next report. Also the mechanism of zinc plating in the membrane will be given in the next report.

6. Summary and Conclusions

The rate limiting step in the deposition of zinc was established by a polarographic method to be the diffusion process. This was effected by demonstrating that the limiting current is proportional to the square root of the height of the mercury column supplying the dropping mercury electrode. This finding eliminates the possibility that dissociation of the zincate ion, or charge transfer, is rate limiting.

From the limiting current and the Ilkovic equation, the diffusion coefficient of zincate in KOH concentrations up to 30% is found to be 8.5×10^{-6} cm^2/sec. At higher concentrations this falls rapidly to 1.5×10^{-6} cm^2/sec. The diffusion coefficient therefore does not follow the Einstein-Stokes law which states that D is inversely proportional to the viscosity.

Examination of absorption isotherms shows that zincate in a separator is present as adsorbed zincate and as free zincate. It is only the latter that participates in diffusion through the separator and in penetration. A low ratio of free internal zincate to external zincate concentration is characteristic of an effective separator.

The concentration of free zincate in a membrane is a non-linear function of the concentrations in the solutions at the two interfaces. Equations have been derived for equilibrium conditions which give the separate internal concentrations of adsorbed and free zincate as a function of external solution concentration. Equations have also been derived for the condition of steady-state diffusion which express internal concentration

of adsorbed and of free zincate as a function of distance from one separator face, and of the external concentration (assuming the concentration at the other face to be negligible). The equations show that concentration of zincate within the separator is a non-linear function of the distance from the faces. From these equations an expression for the flux of zincate through the separator is derived. When the flux of zincate through the external solution to those regions of the zinc electrode in contact with the separator falls below the flux through the separator, then penetration of the separator is initiated.

The quantity of zincate adsorbed per molecule of regenerated cellulose is such as to indicate that zincate is held only at the ends of the chain.

At low zincate concentrations, surfactants displace zincate from the adsorption sites, and thus decrease zincate adsorption. At high zincate concentrations, zincate displaces the surfactant and the influence of the surfactant disappears.

As the liquid level in cells fluctuates, the separator tops dry out and crystals, shown to be ZnO or $Zn(OH)_2$, are deposited in this portion of the membrane. Cracks develop in the separator in the vicinity of the crystals. It has long been known that cellulose separators deteriorate first in the portions above the electrolyte level and between the upper and lower limits of fluctuation of the electrolyte level. This cracking around the deposited crystals may prove to be an important factor in separator deterioration.

An apparatus for measuring zincate flux under steady-state and non-steady-state conditions was constructed and put into operation. The equipment is novel in that reduction of zincate at one face holds the zincate concentration at zero, and in that rotation of the membrane eliminates the boundary layer effect at the other face.

The increase in overpotential in galvanostatic charging of a plate which has experienced shape change is greater than would be expected from the decrease in geometric area. This indicates that real area has also decreased. This finding is consistent with a self accelerating process with the following steps.

Minor decrease in geometric area.

Increase in current density.

Increase in overpotential:

Conversion from deposition of mossy zinc to dendritic zinc and loss of real surface.

Greater increase in real current density.

Greater increase in overpotential and coarser deposit.

The form of zinc deposited on a substrate is independent of the substrate metal.

A theory is presented which accounts for the form of the zinc deposit. At low overpotential zincate can diffuse readily to regions near the ends of whiskers, but zincate is exhausted before it can penetrate within the mass. Consequently, deposition is simultaneously activation controlled at the whisker tips, concentration polarized within the moss, and under mixed activation and diffusion controls in an intermediate region near the tips.

This part of the proposed mechanism thus accounts for the phenomenon of deposition being diffusion controlled at low concentration overpotential.

When the overpotential is raised above a critical value, the intermediate region disappears because the deposition rate at the tips increases. The diffusion layer moves out beyond the plane of the tips. The entire deposit now becomes diffusion controlled causing a change from mossy to dendritic structure. The exchange current density for zinc in 44% KOH was measured and found to be 0.006 A/cm^2 (assuming a roughness factor of 2).

7. PROGRESS FOR THE NEXT QUARTER

1. Continue kinetic studies of zinc deposition with special emphasis on the use of the rotating disc technique to establish the parameters needed for comparing the proposed mechanism of deposition with experimental findings.
2. Extend the studies of zincate flux in separators to a range of materials.
3. Construct the cells required by the contract.
4. Complete the Final Report.

Fig. 1 Zincate Polerograms

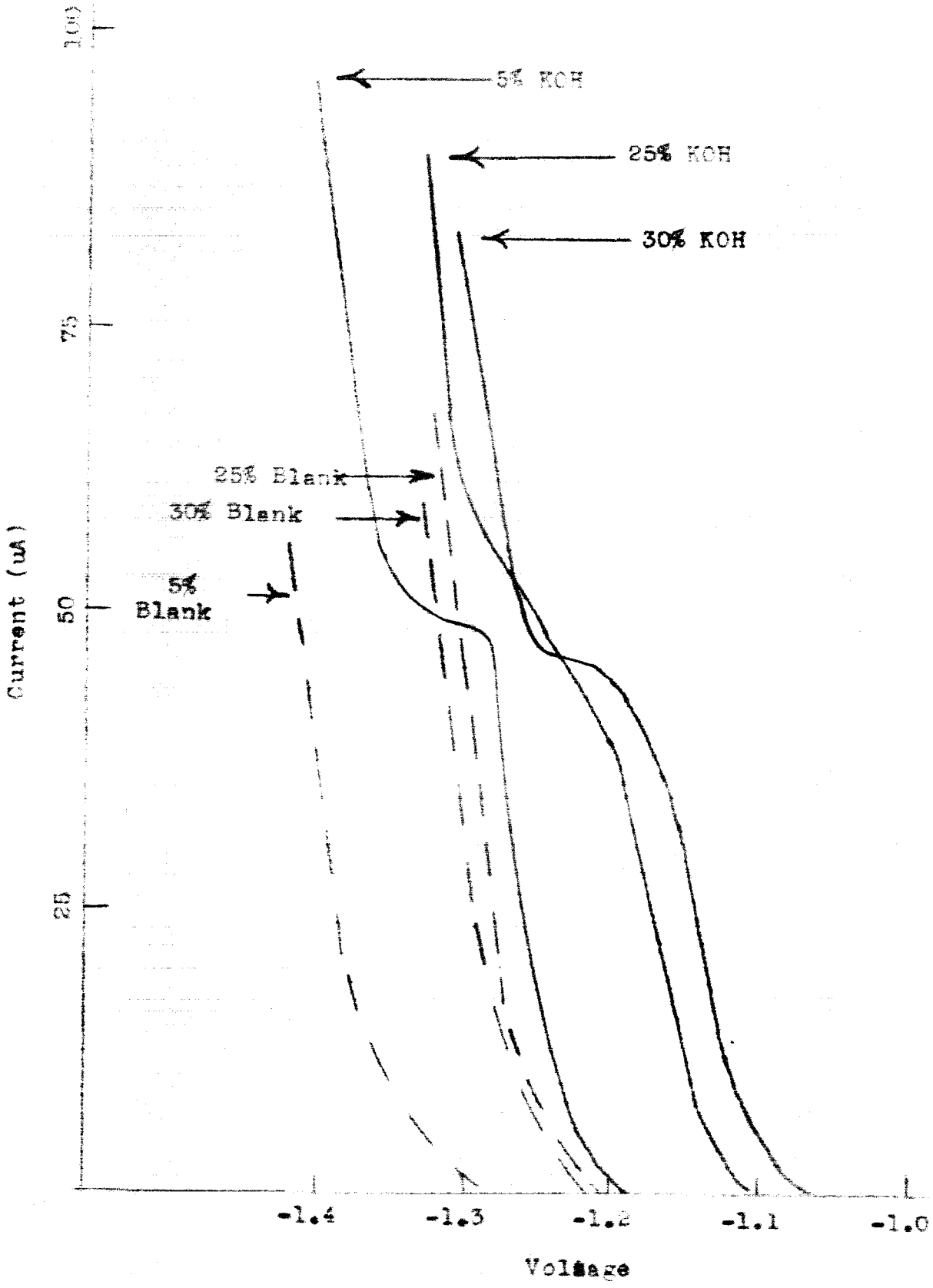

Fig. 2 Zincate Polarograms

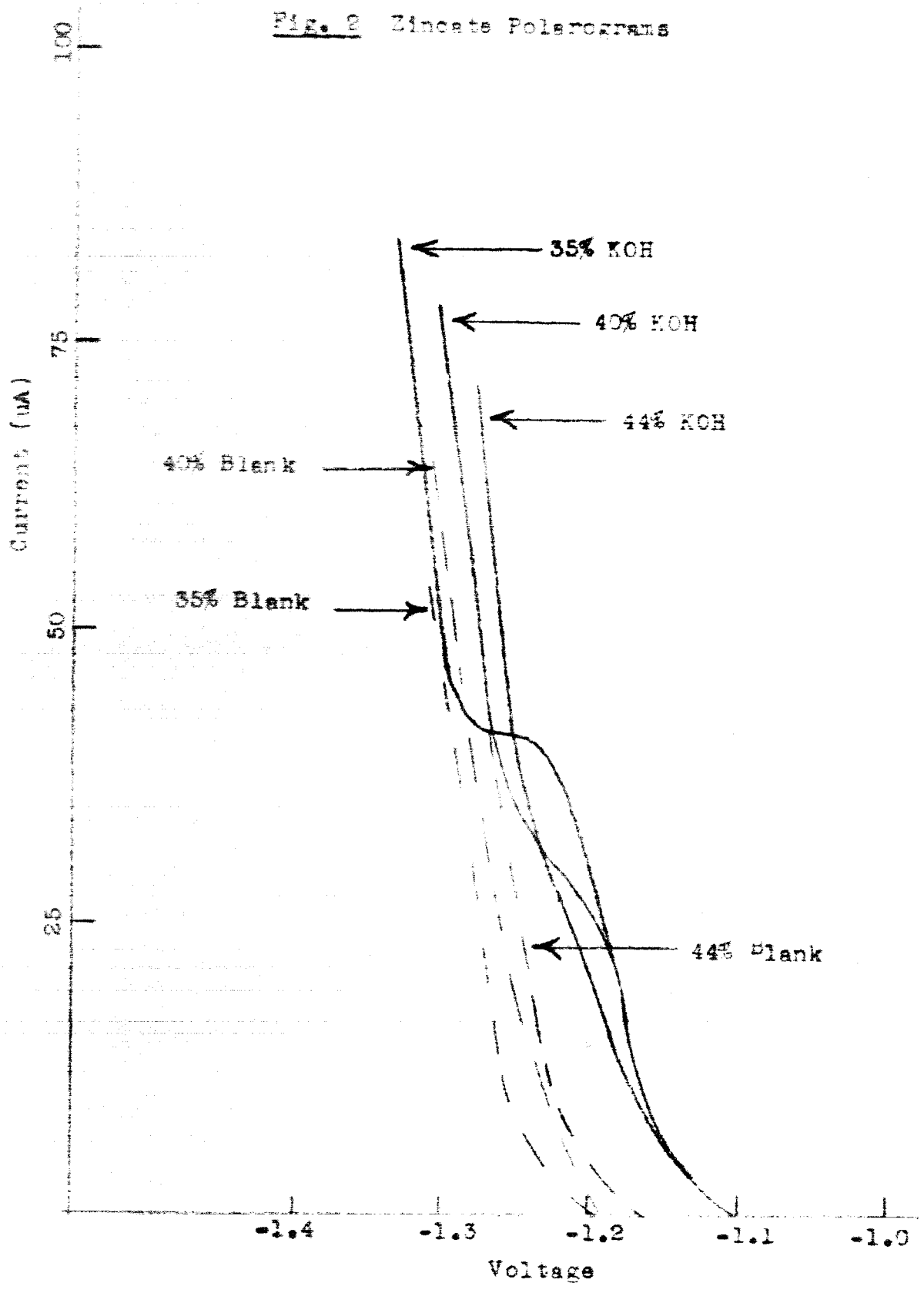

Fig. 3 The Effect of Mercury Pressure on the Limiting Current

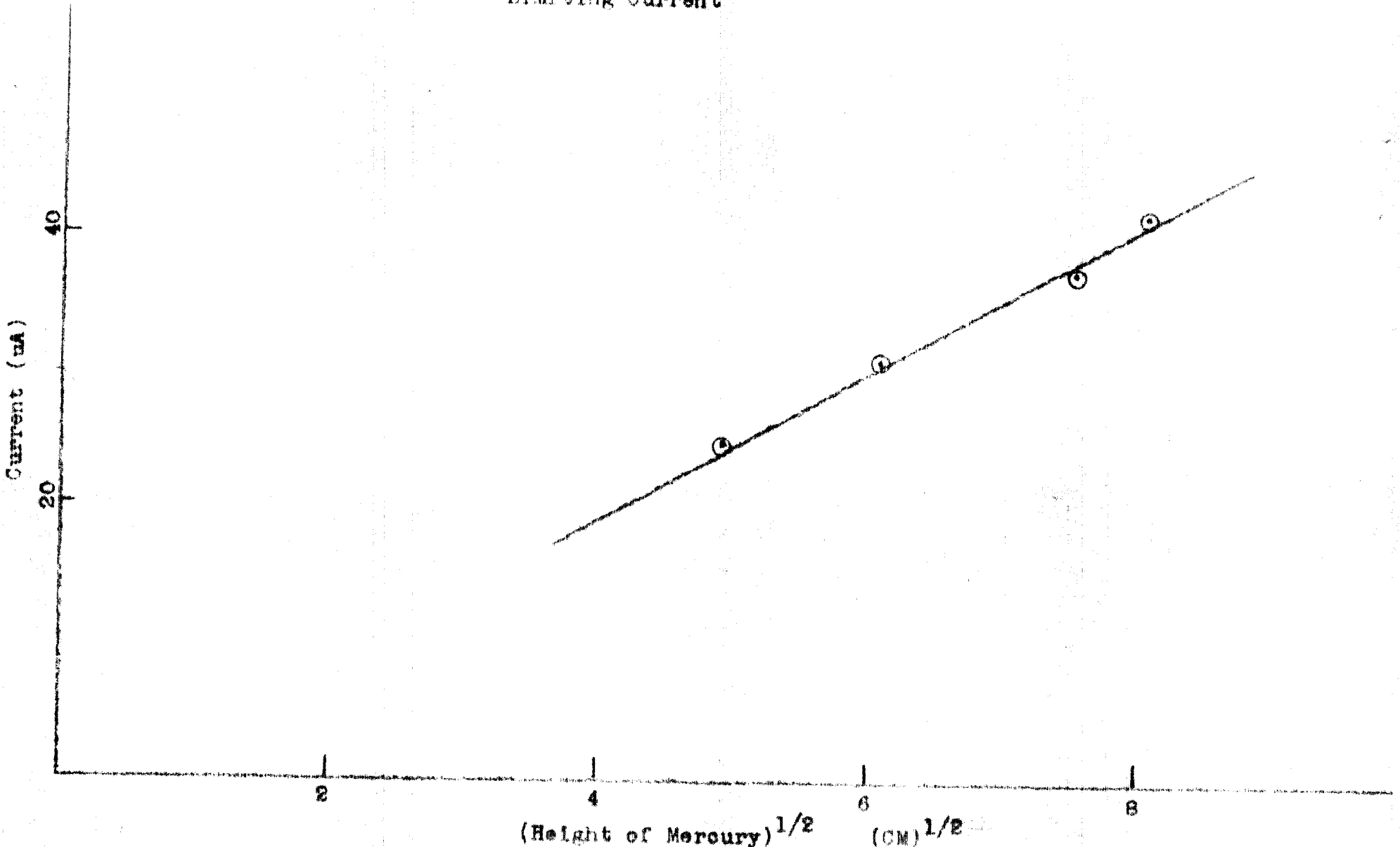

Fig. 4 Variation of the Half-Wave Potential of Zinc with KOH Concentration

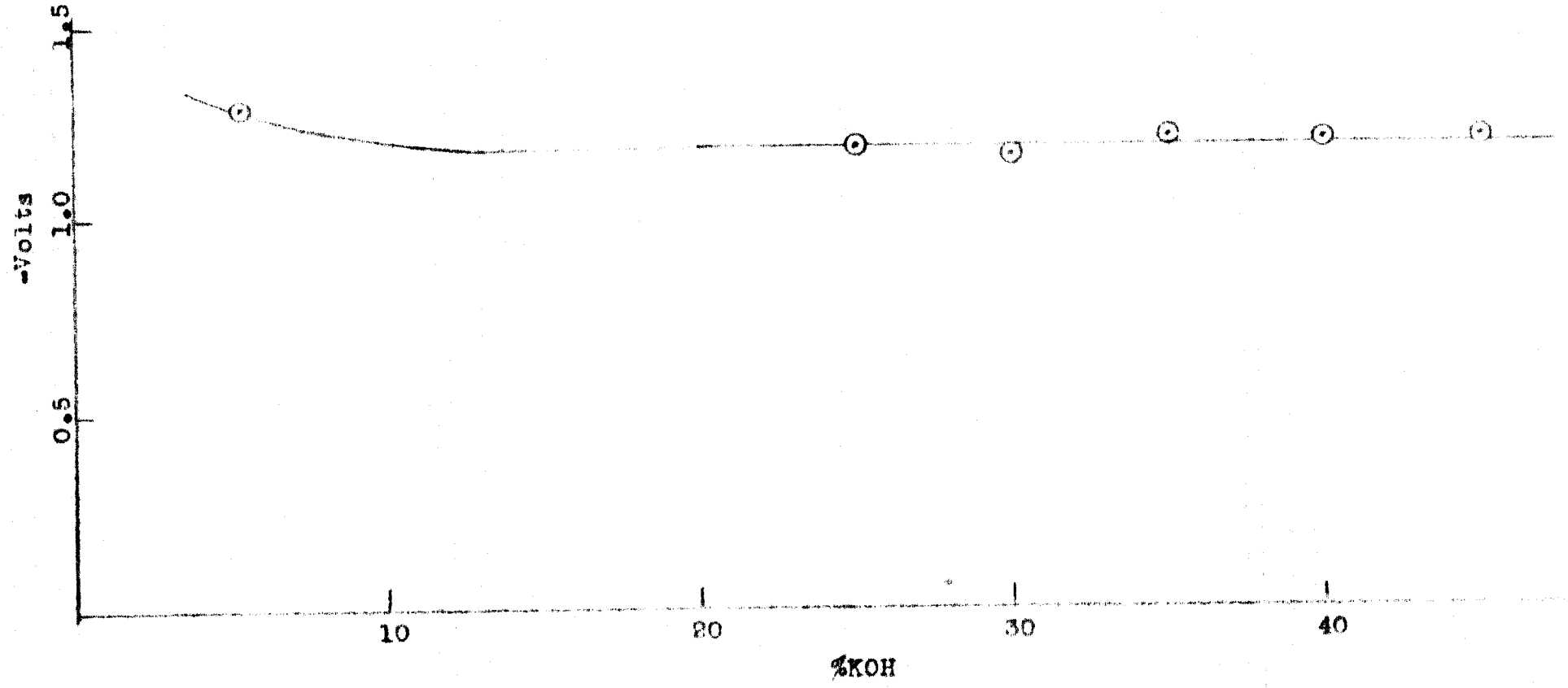

Fig. 5 Effect of KOH Concentration on Limiting Current Density for Zincate

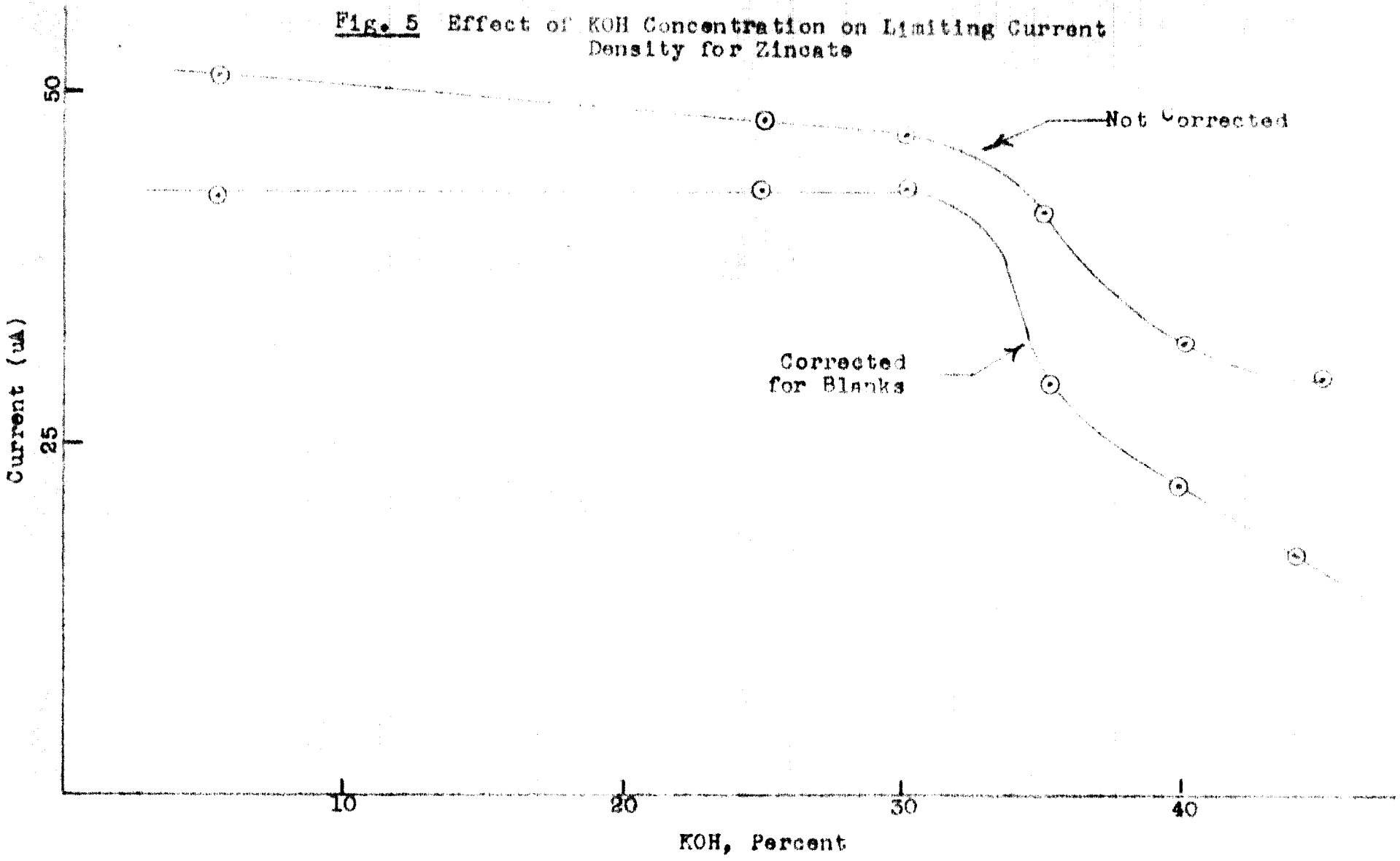

Fig. 6 Zincate Diffusion Coefficient from the Ilkovic Equation as a Function of KOH Concentration

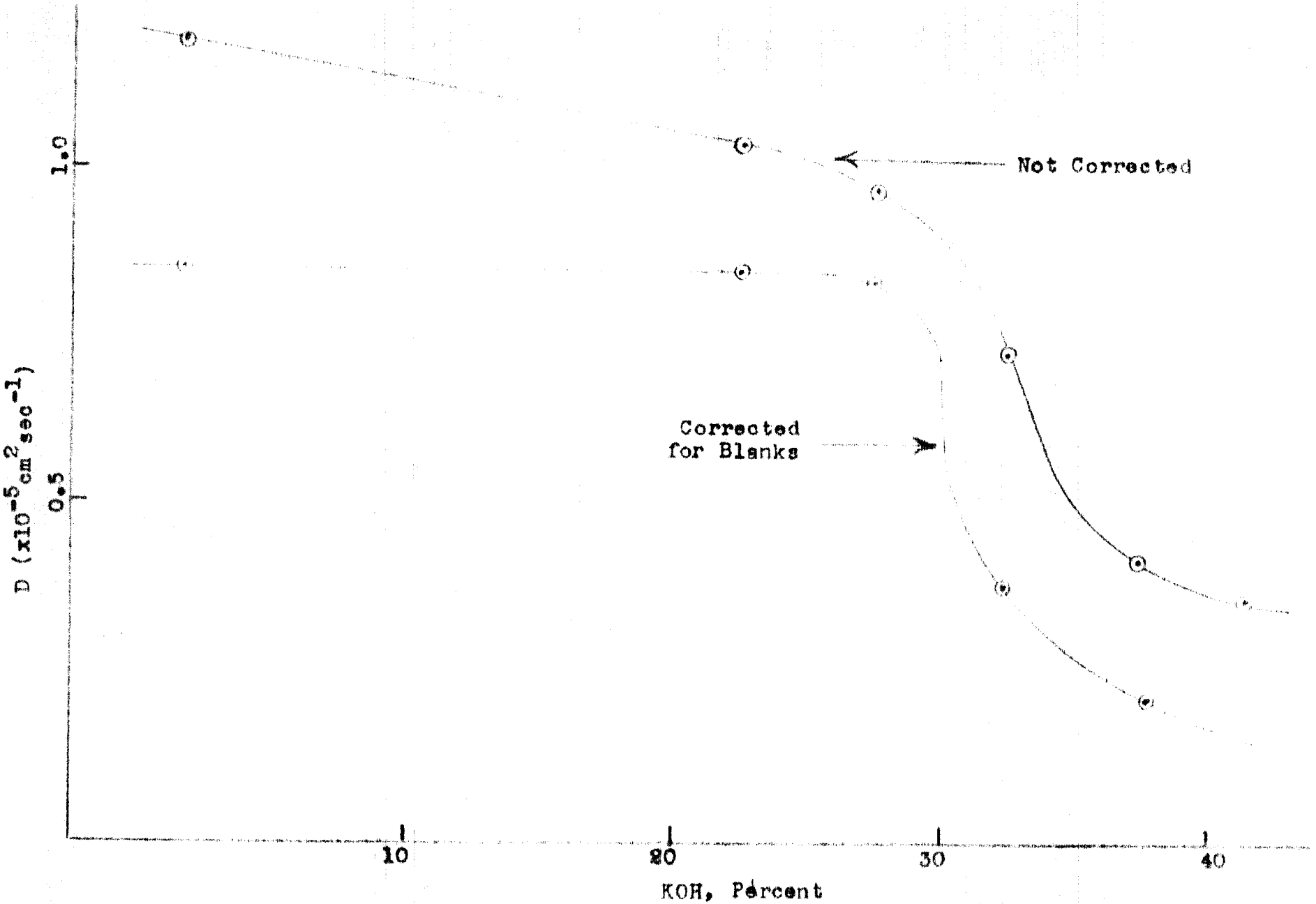

Fig. 7 Zincate Diffusion Coefficient from the Ilkovic Equation vs. the Reciprocal Viscosity

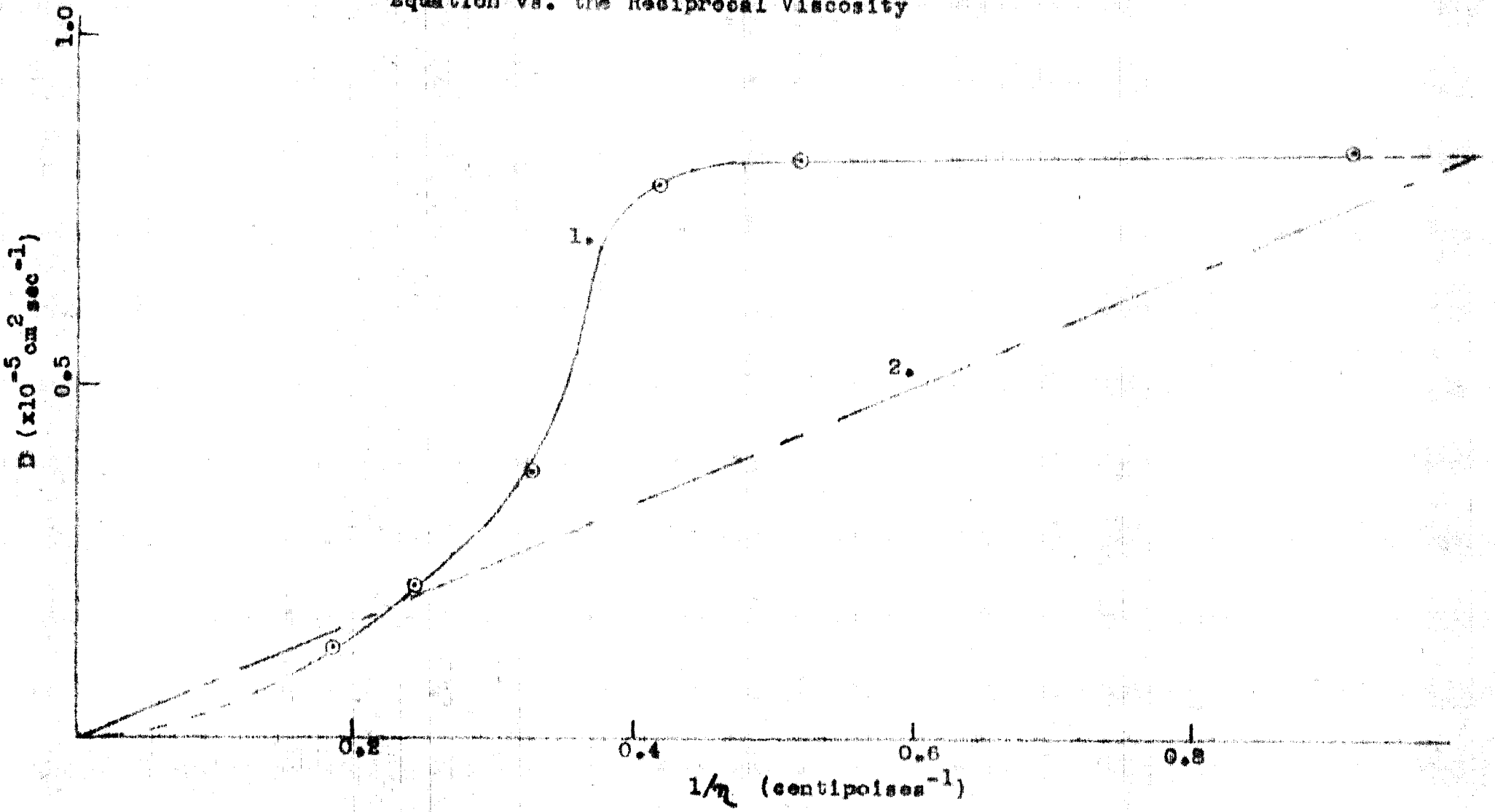

Fig. 8 Components of the Absorption Isotherm

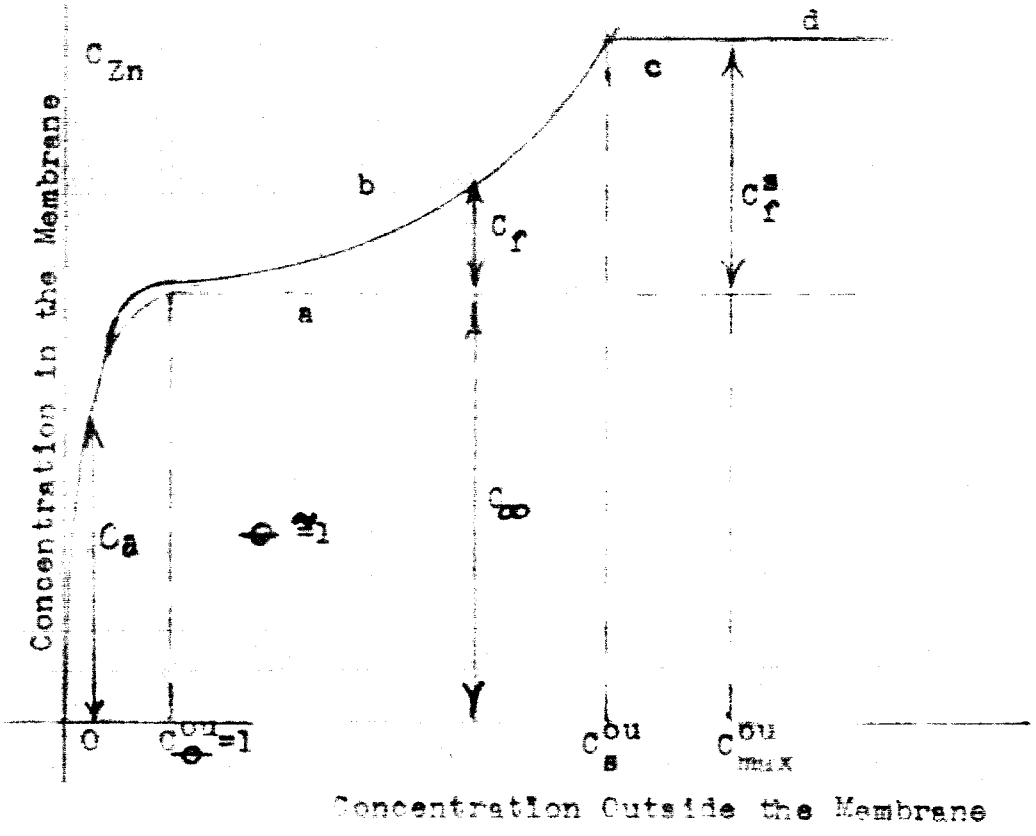

Fig. 9 Calculated concentration of free Zincate in Cellophane as a Function of Outside Concentration

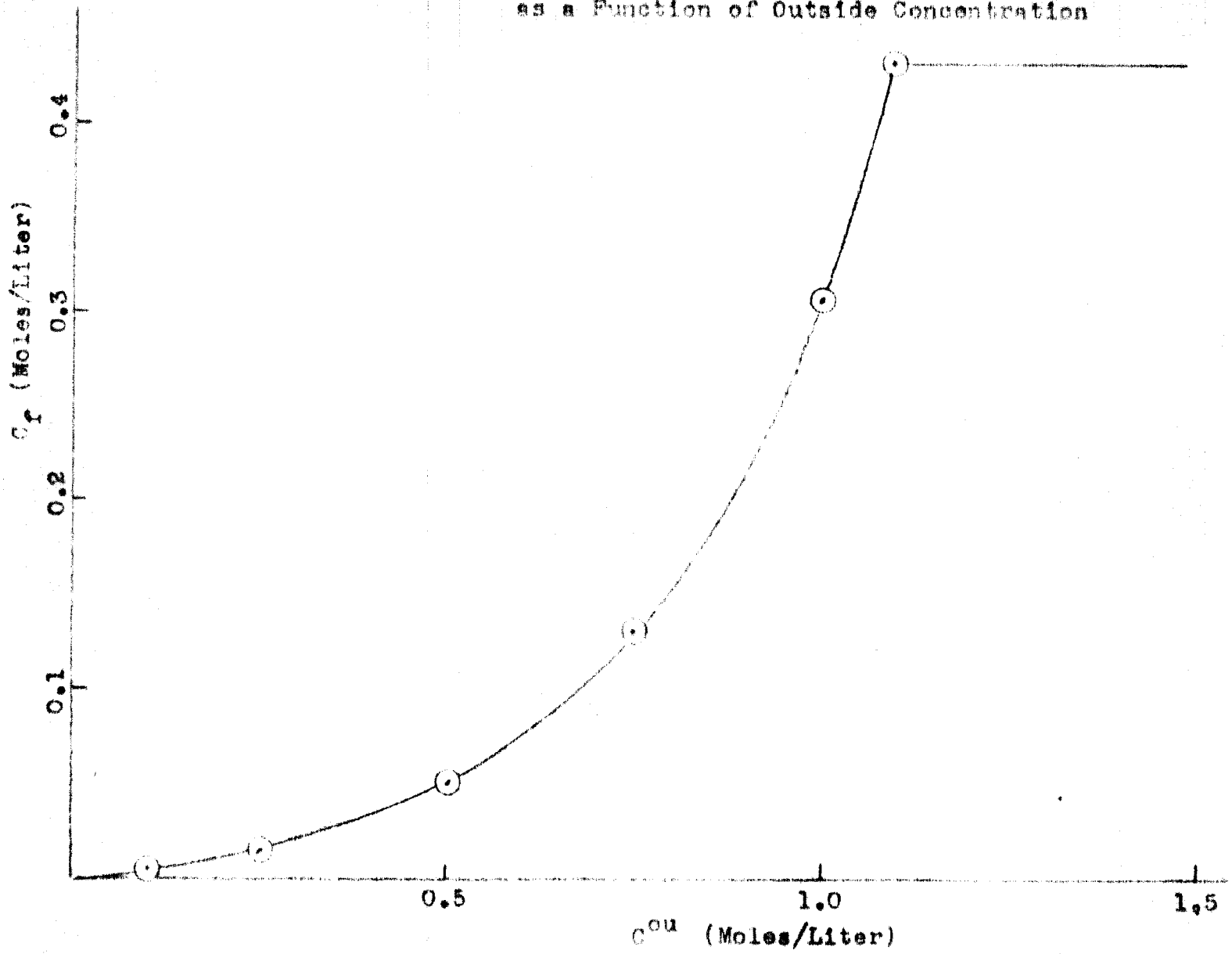

Fig. 10 Calculated Inner Concentration of Zincate in Cellophane as a Function of Outside Concentration

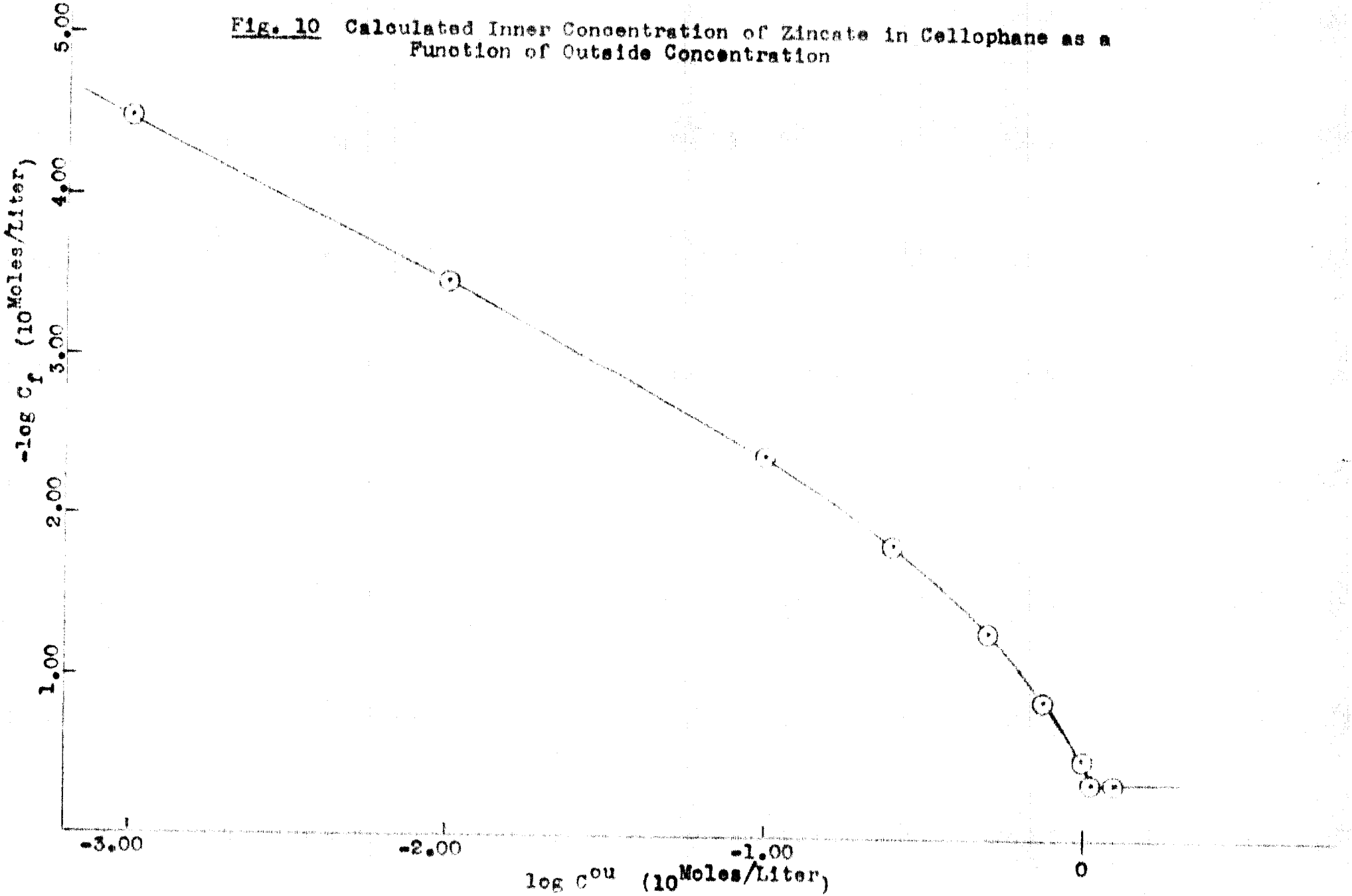

Fig. 11 Theoretical Curve of Zincate Absorption in Cellophane Compared with Experimental Points.

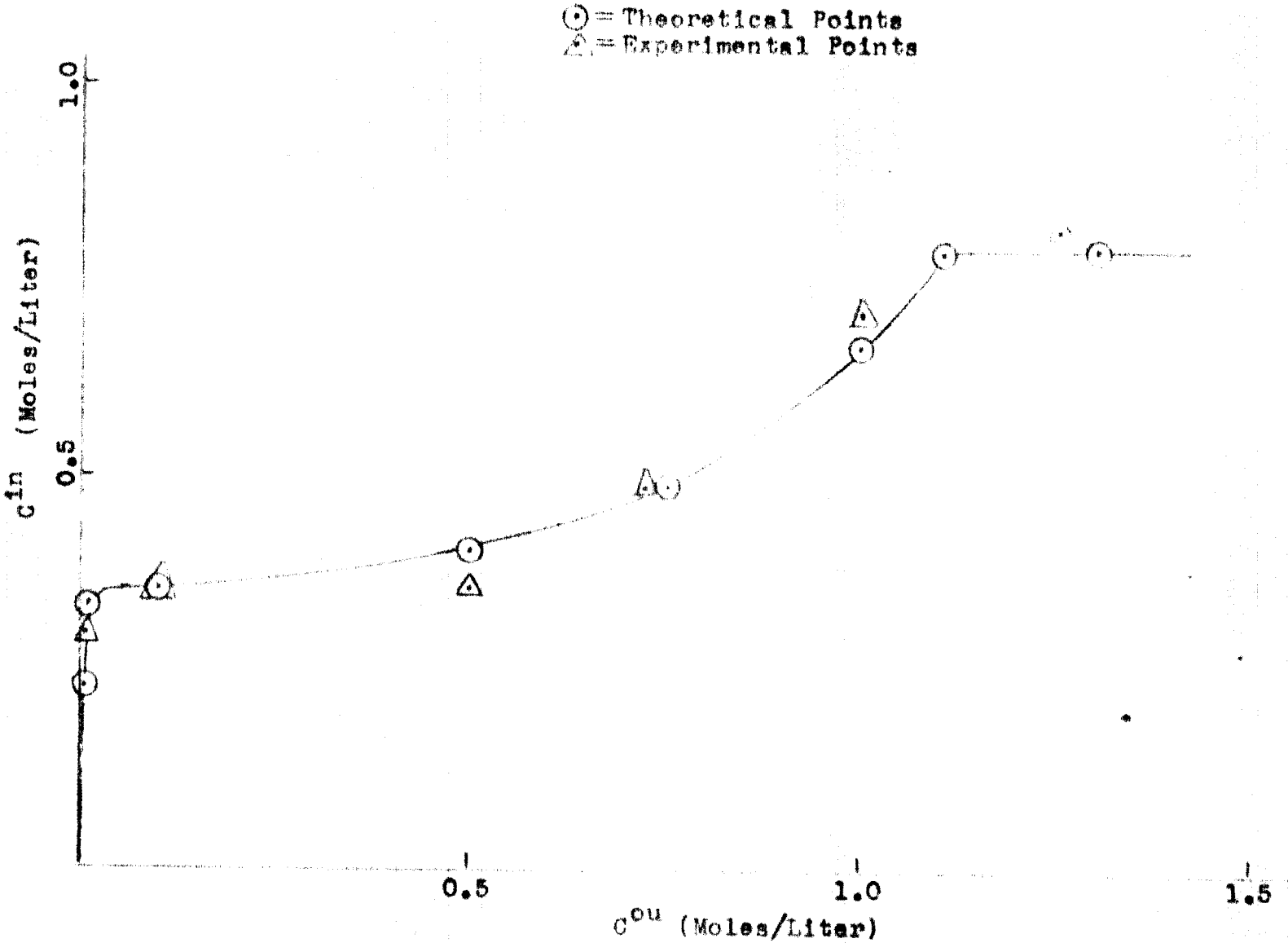

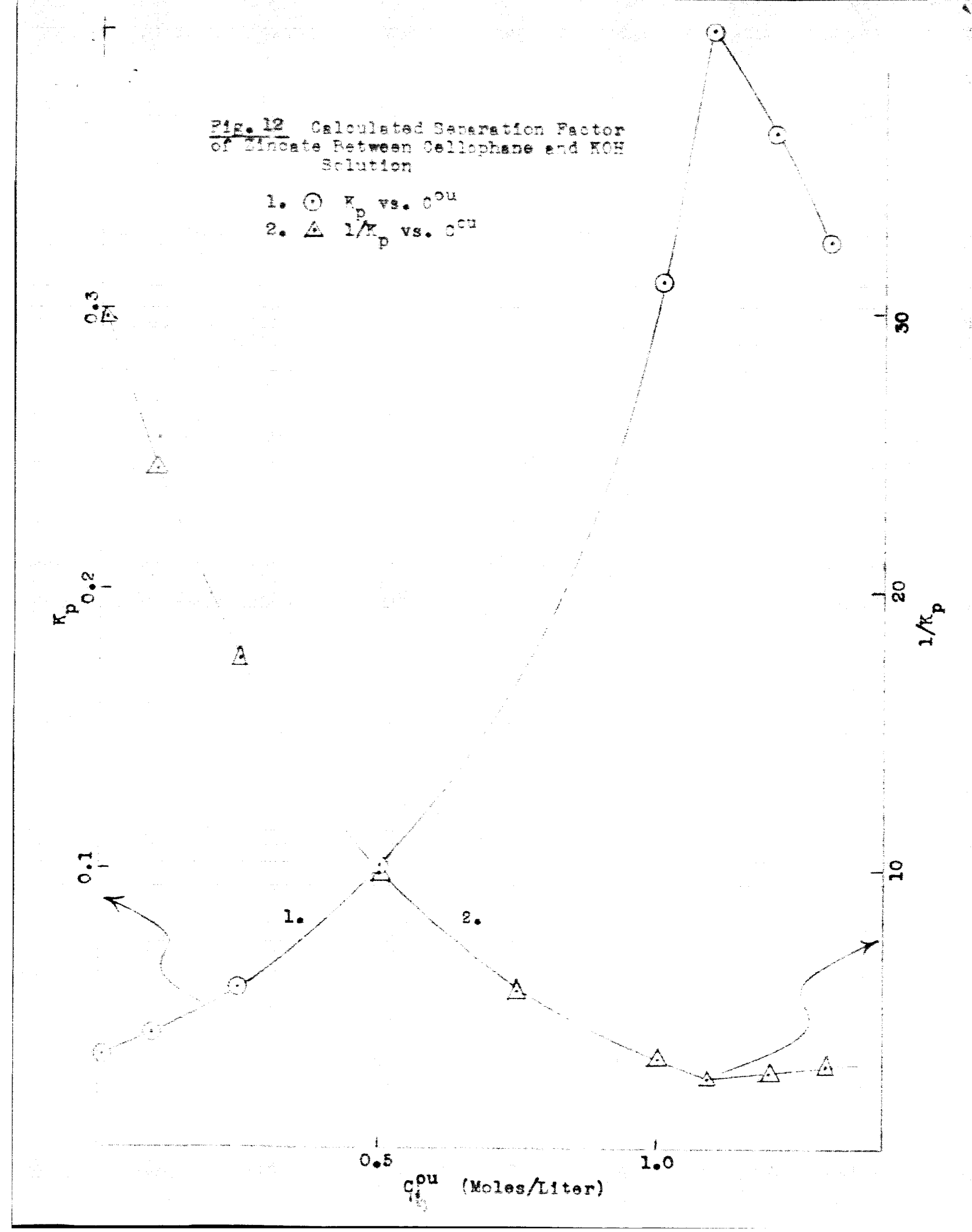
Fig. 12 Calculated Separation Factor of Zincate Between Cellophane and KOH Solution
1. ⊙ K_p vs. C^{Cu}
2. △ $1/K_p$ vs. C^{Cu}
0.3
0.2
0.1
K_p
30
20
10
$1/K_p$
1.
2.
0.5
1.0
C^{Cu} (Moles/Liter)

Fig. 13 Variation of Fick's Diffusion Coefficient of Zincate in the Cellophane as a Function of Concentration

1. D_f/D_o vs. C^{ou}

2. D_f/D_o vs. C_f

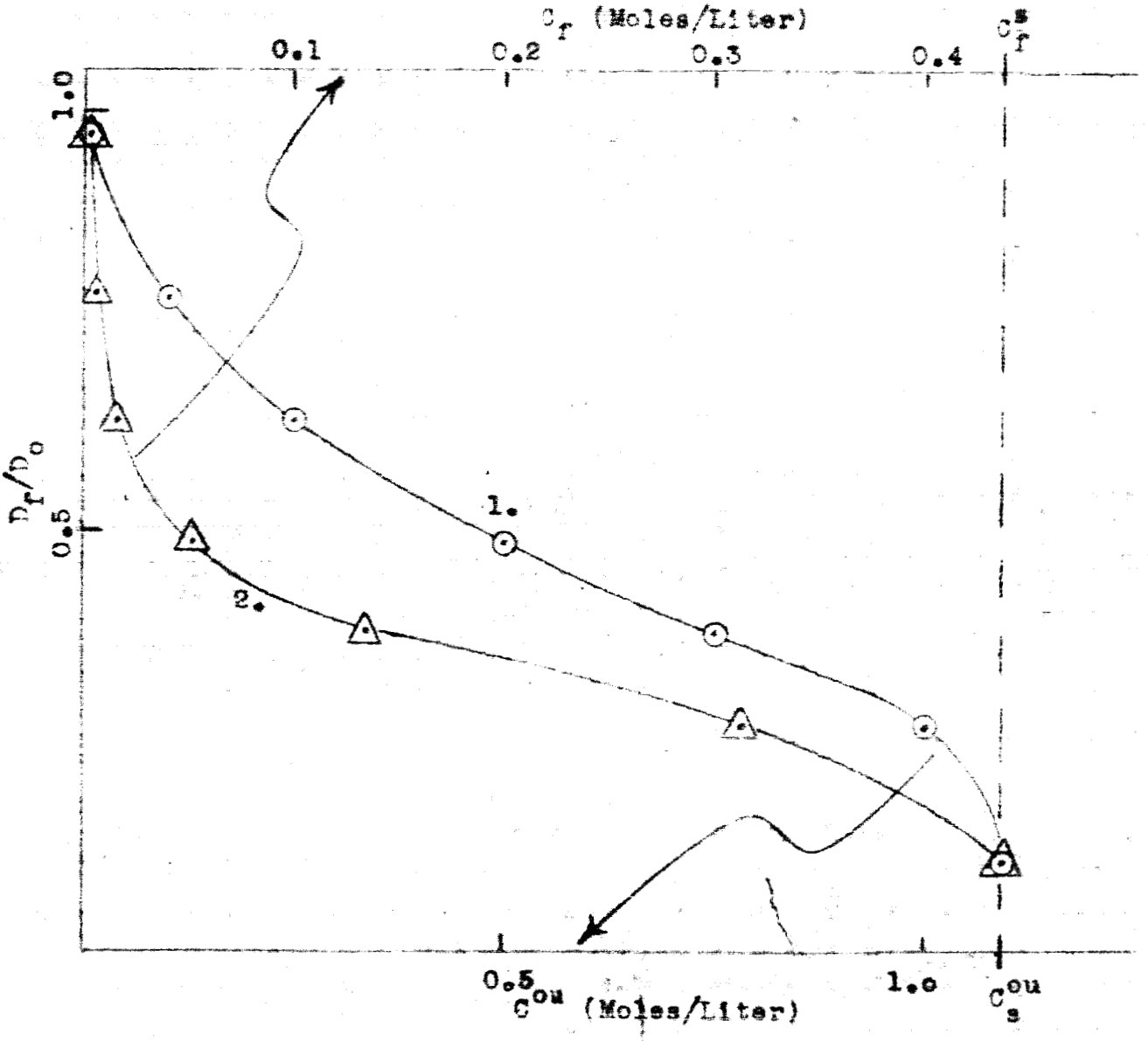

Fig. 14 Distribution of Total Zincate Content in the Cellophane Membrane During the Diffusion Through It

⊙ C^{ou}=1.09 Moles/Liter=C_s^{ou}
⊡ C^{ou}=0.50 Moles/Liter
● C^{ou}=10^{-1} Moles/Liter
▲ C^{ou}=10^{-2} Moles/Liter
■ C^{ou}=10^{-3} Moles Liter

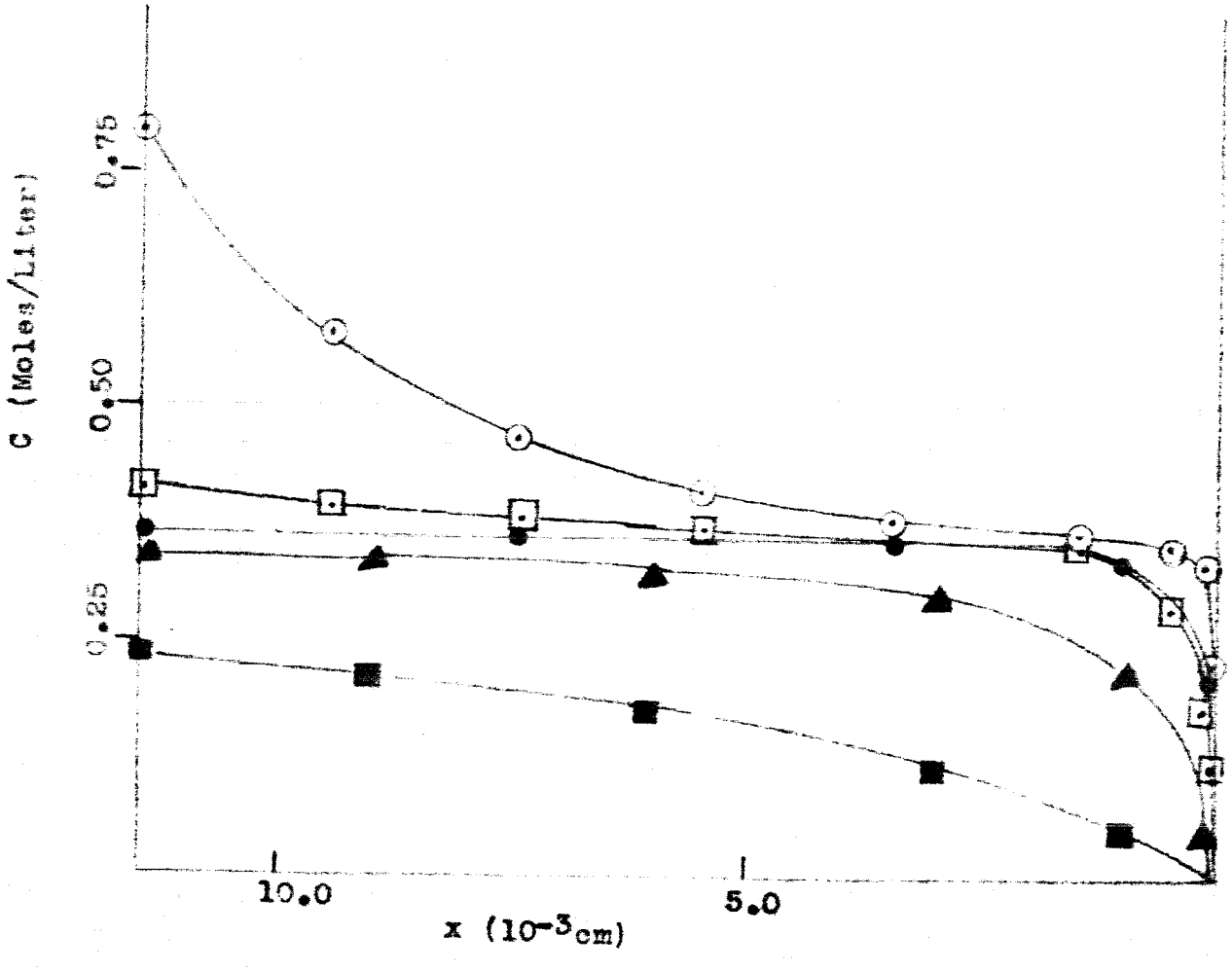

Fig. 15 The Influence of Surfactant on the Absorption Isotherm of Zincate

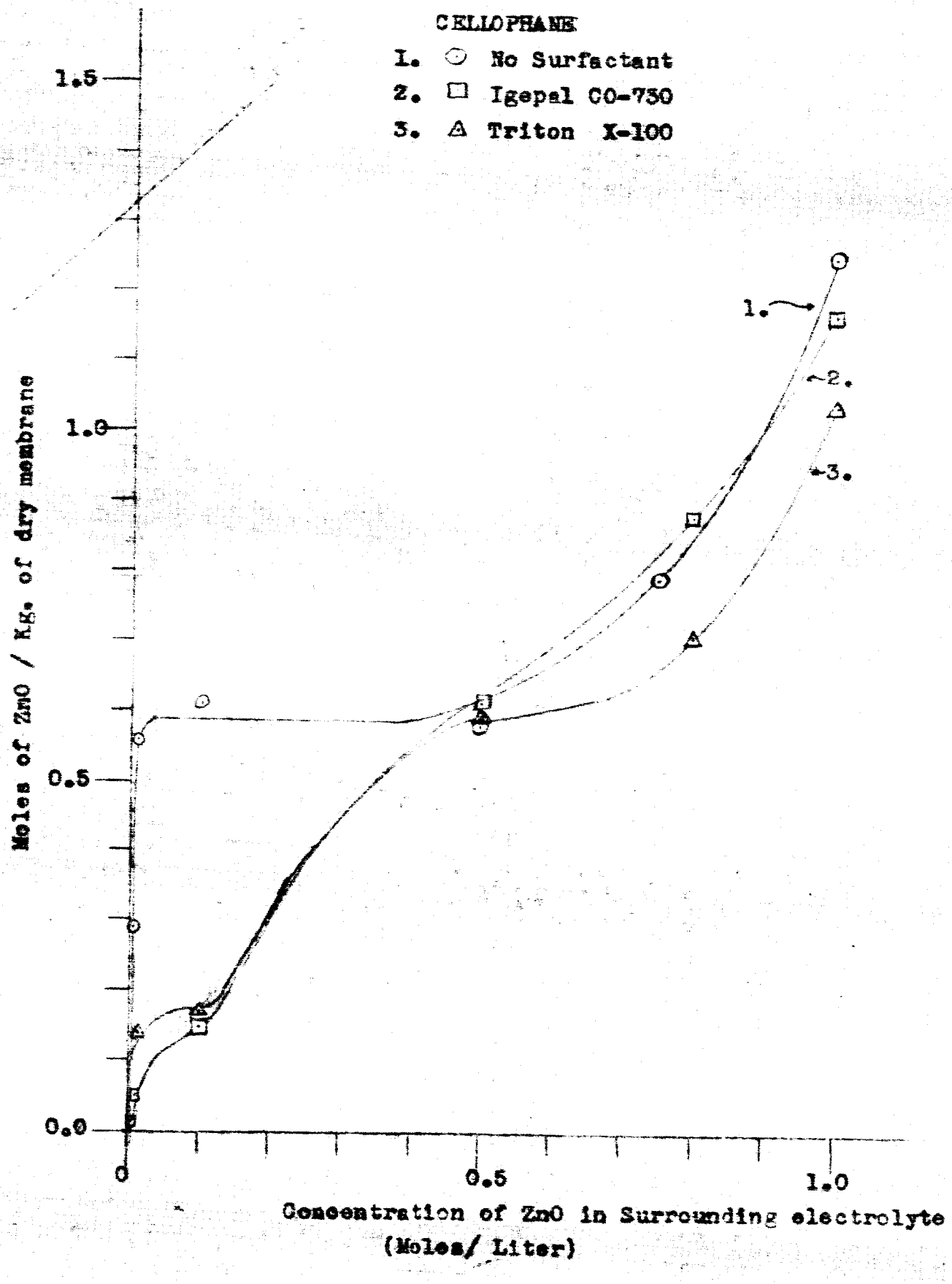

Fig. 17 Zincate Permeability Transient Through a Membrane

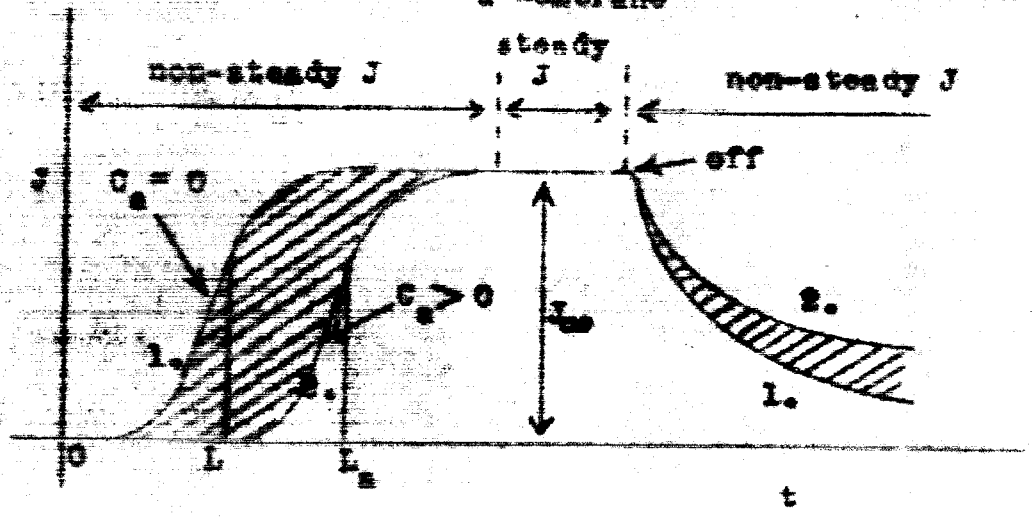

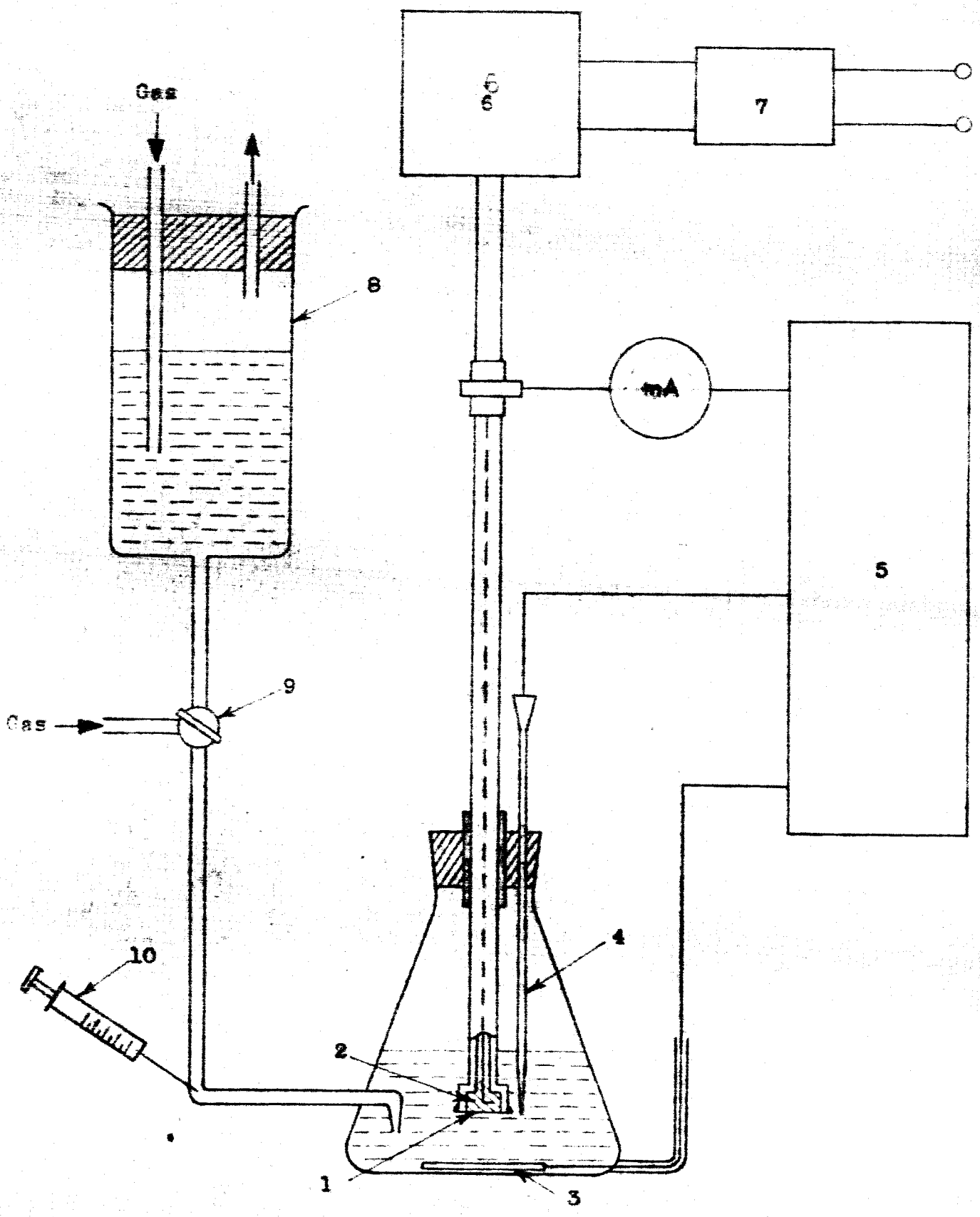

Fig. 18 Apparatus for measurement of the diffusion transients of zincate through the separators

Fig. 19
Polarization curves of shape changed zinc electrodes

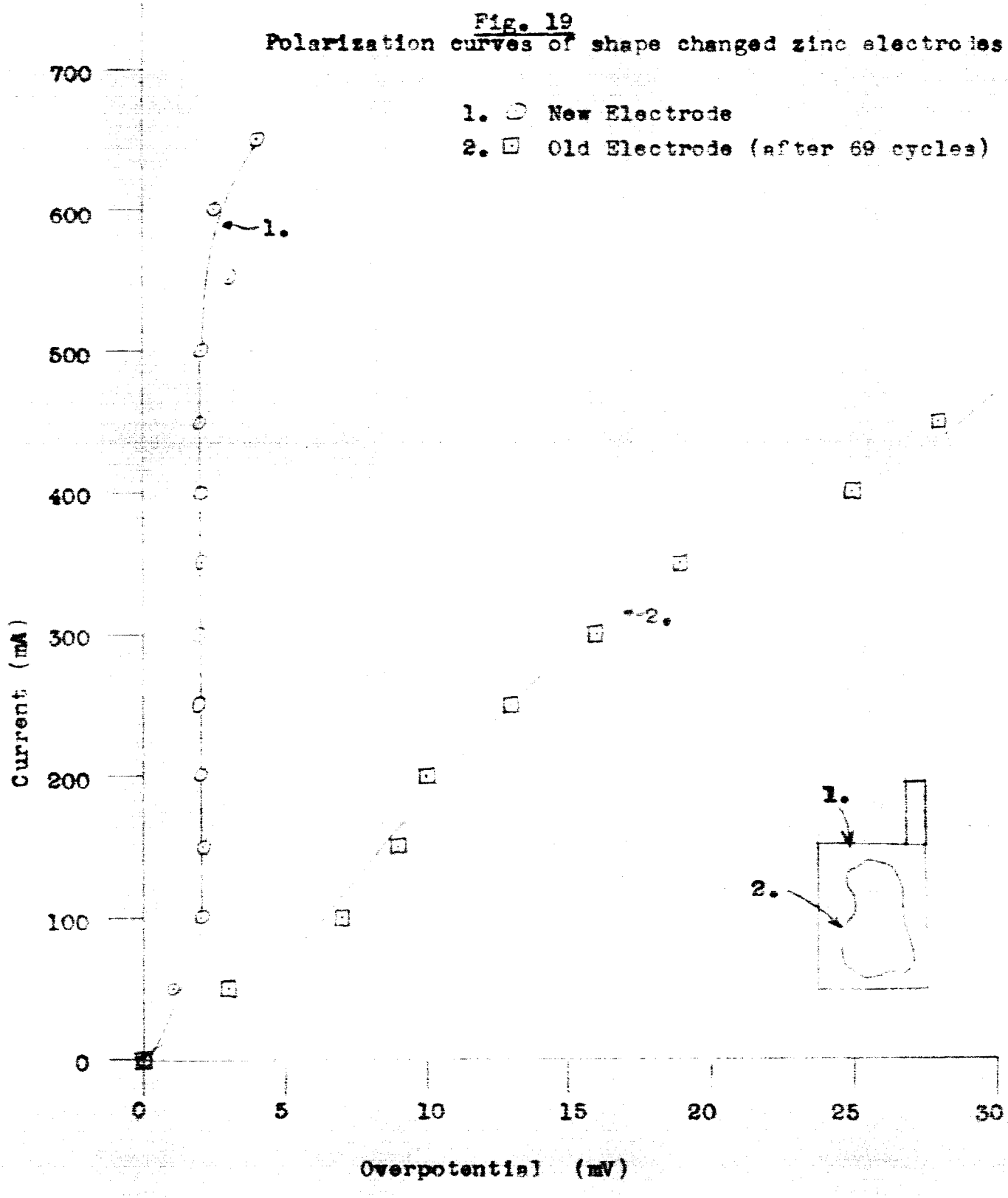

Fig. 20 Voltamperometric Plating of Zinc from 35% KOH Saturated with Zincate under N_2 onto Ag Rotating at 8.8 rev/sec.

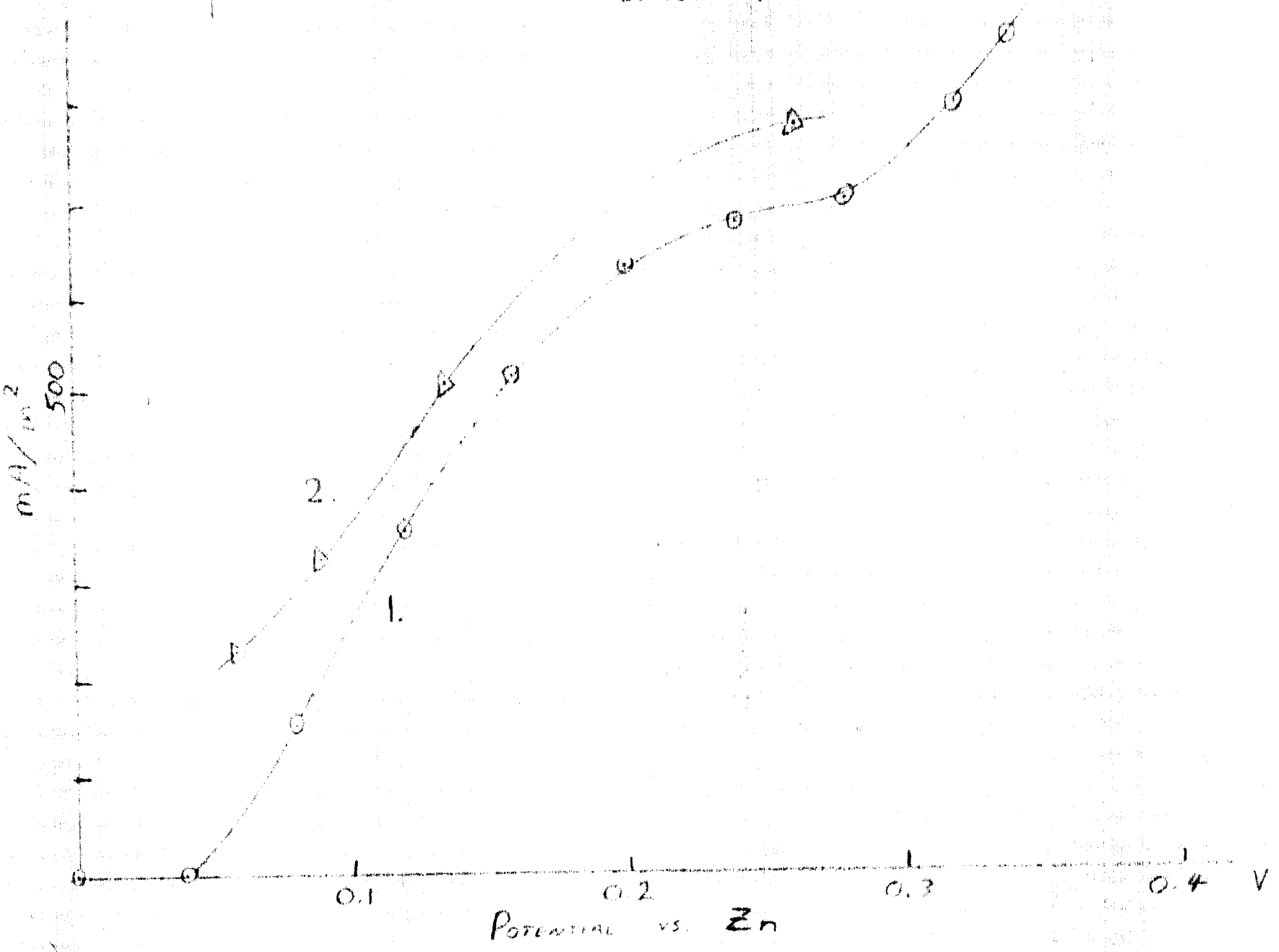

Fig. 21 Potentiostatic Plating of Zinc from 35% KOH Saturated with Zincate onto Ag Rotating at 8.8rev/sec. Current vs. time for various overpotentials.

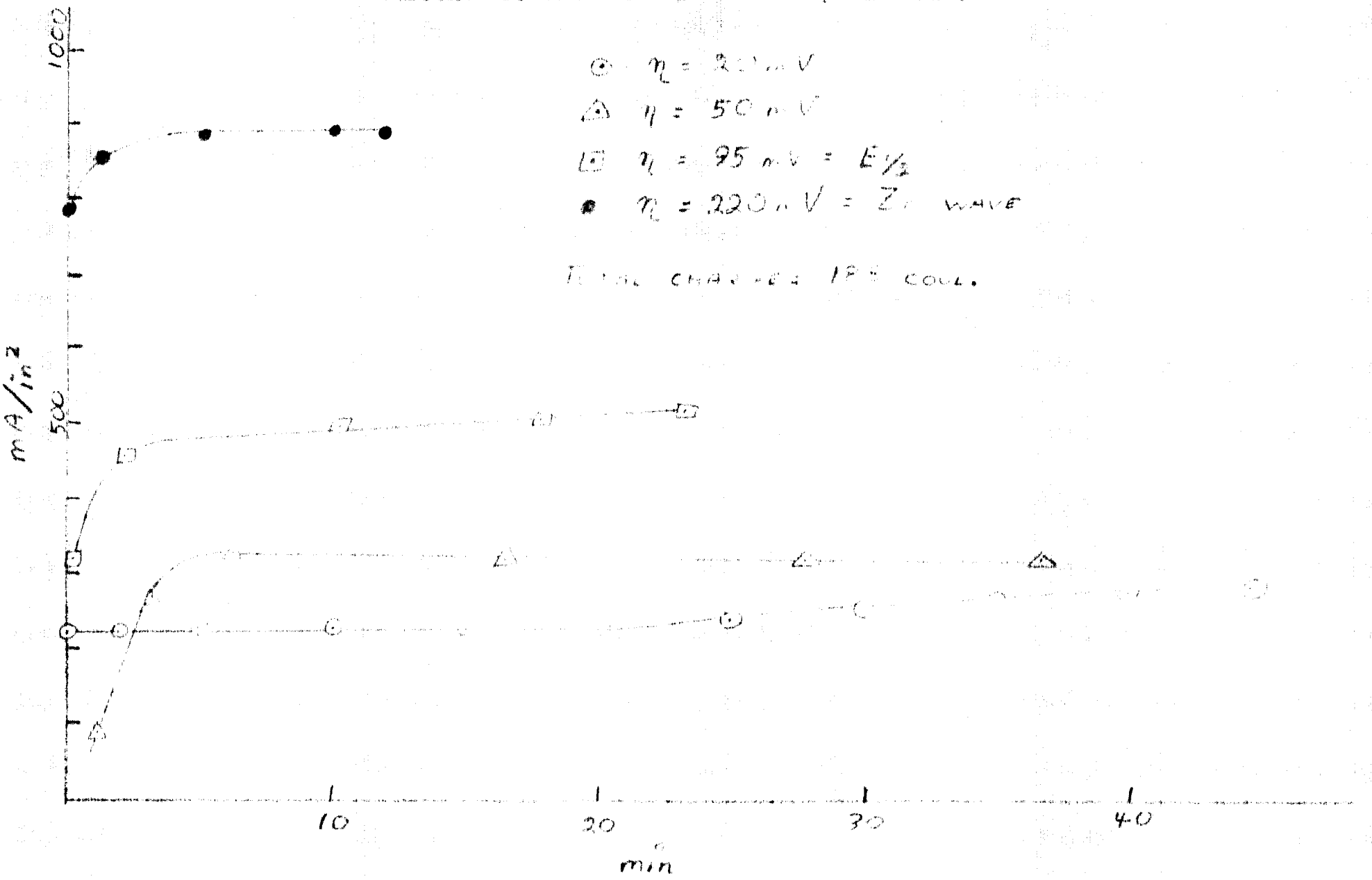

Fig. 22 Limiting Current of Zinc Plating on Ag Rotating at 8.3 rev/sec. in 35% KOH as a Function of Zincate Concentration

Fig. 23. Potentiostatic Plating of Zinc from 35% KOH on Ag Rotating at 8.8 rev./sec.

Overpotentials were as indicated, which correspond to the limiting current potentials determined from the polarization curve.

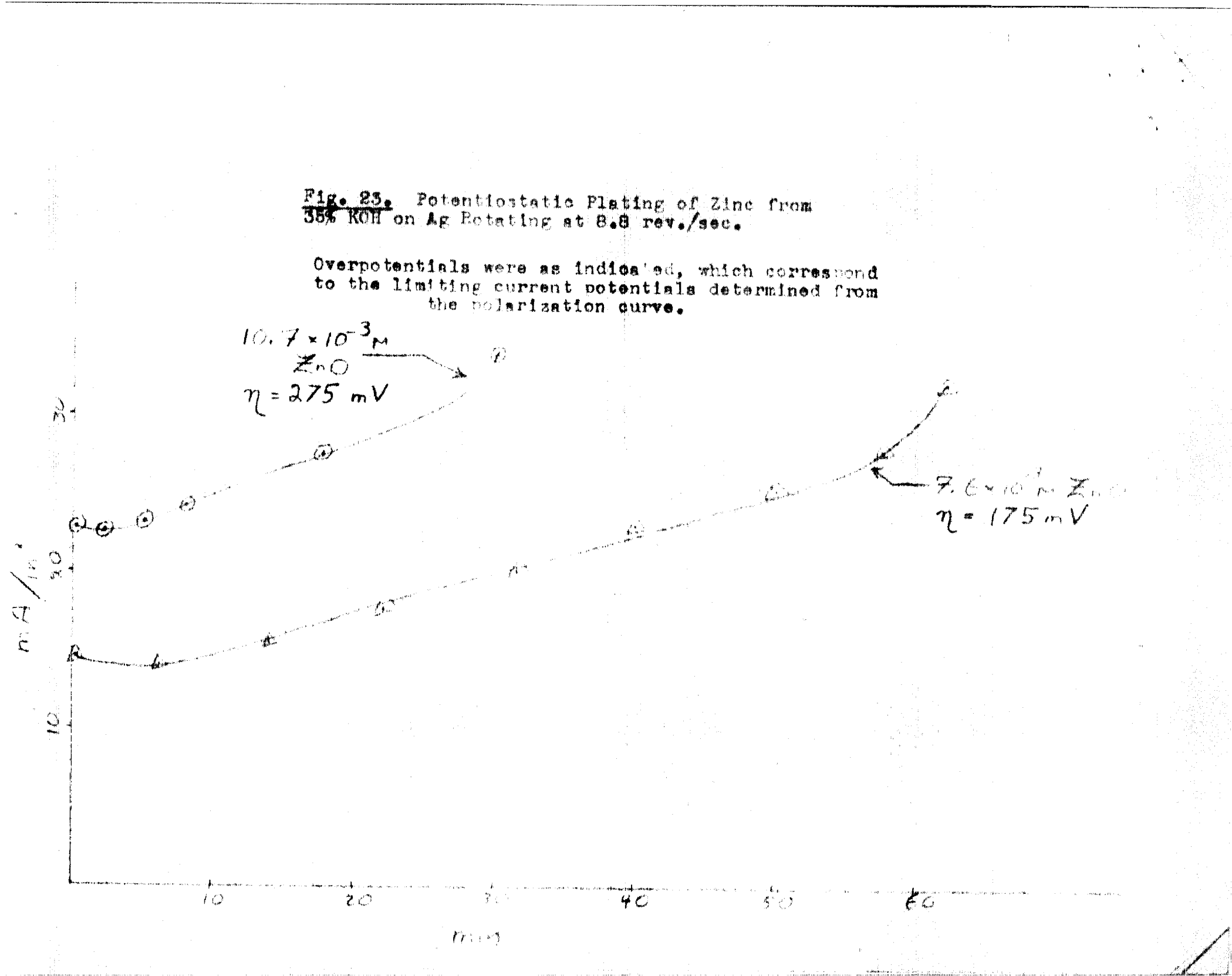

Fig. 24. Limiting Current of Zinc Plating of 7.6×10^{-3} M ZnO in 35% KOH on Silver Rotating Disc as a Function of the Rotation Speed

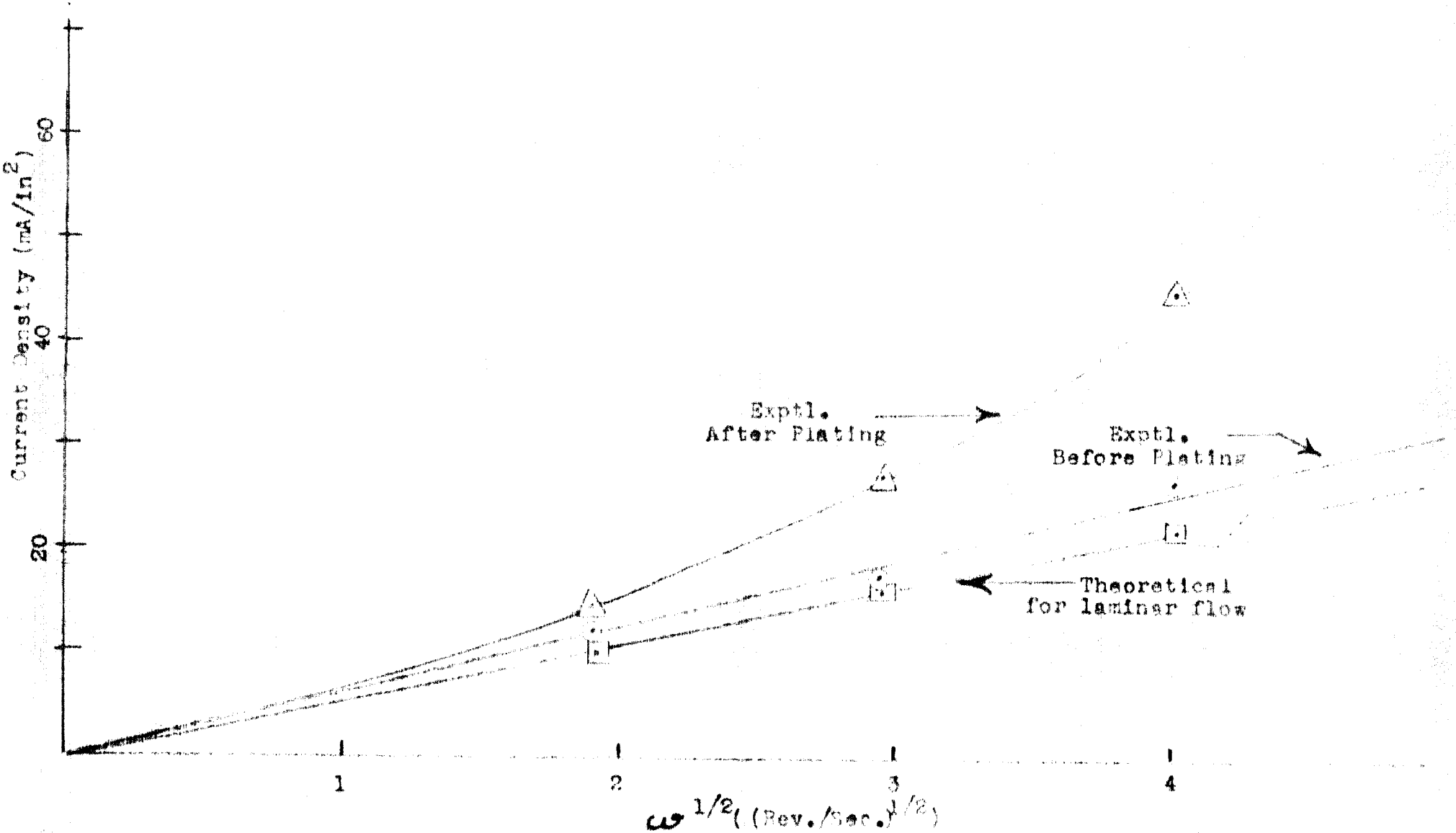

Fig. 25 Theoretical and Experimental Limiting Currents of Zinc Plating on Ag Rotating Disc in 35% KOH as a Function of Zincate Concentration

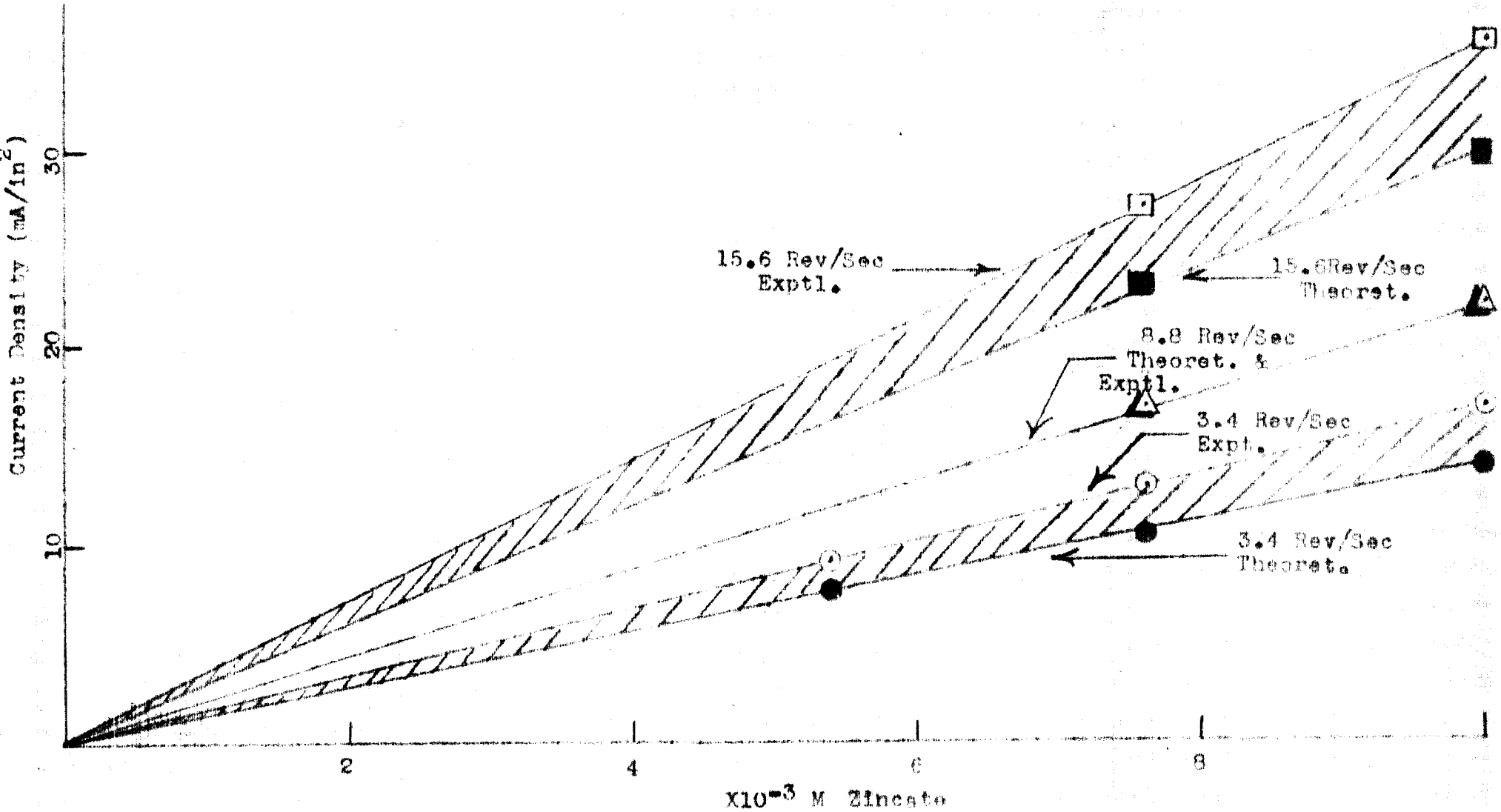

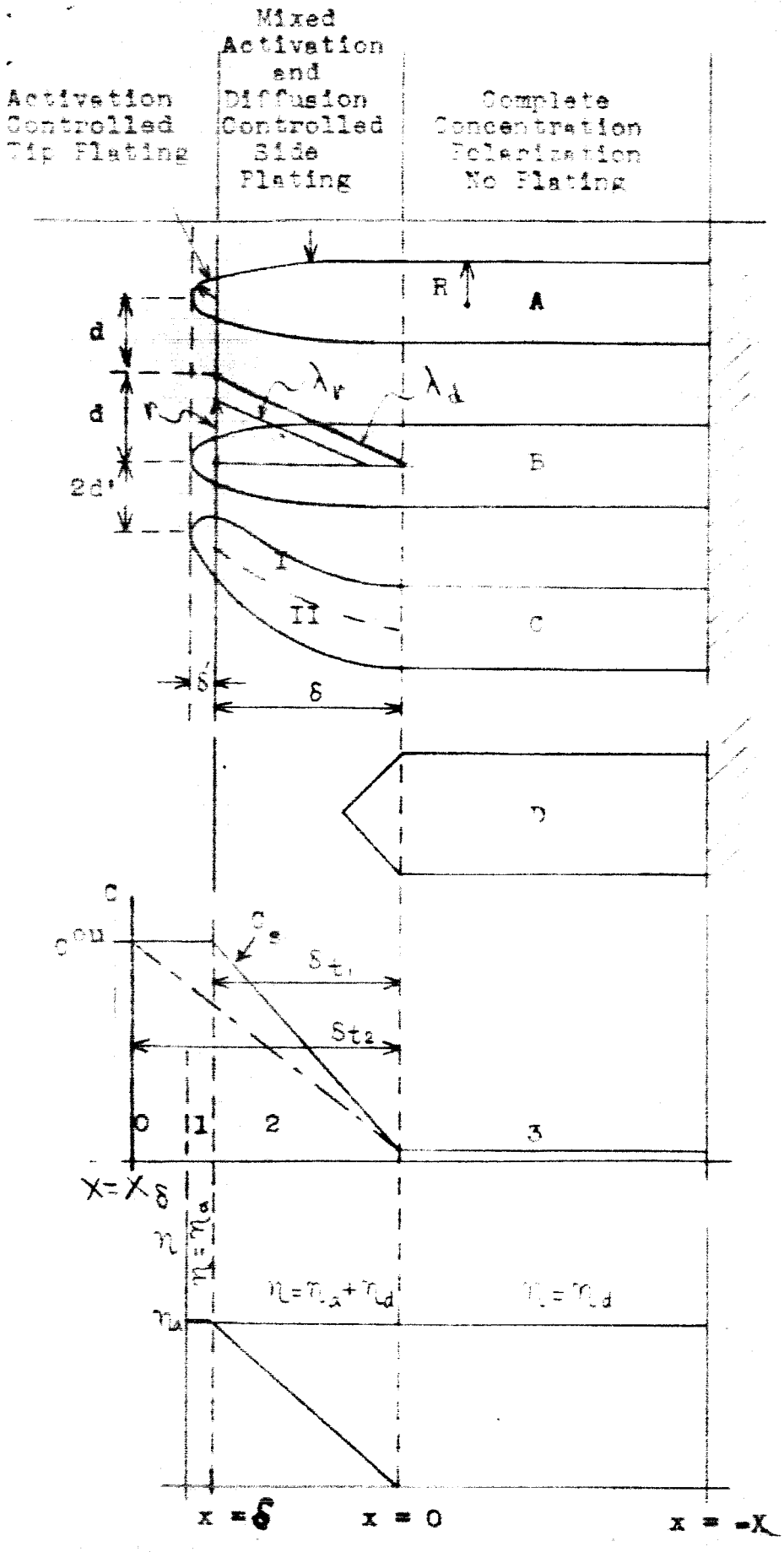

Fig. 26 a - Diagramatic representation of selfregulating mechanism of wisker plating in a mossy deposit.

Fig. 26 b - Dendritic growth.

Fig. 26 c - Concentration gradient. Condition of mossy plating:

$$\frac{dX_\delta}{dt} = \frac{dl}{dt} \quad ; \quad x_\delta = \delta + X$$

Dendritic plating:

$$\frac{dX_\delta}{dt} > \frac{dl}{dt}$$

Fig. 26 d - Distribution of components in a mossy deposit.

Fig. 26 - Model of mossy and dendritic plating from the solution.

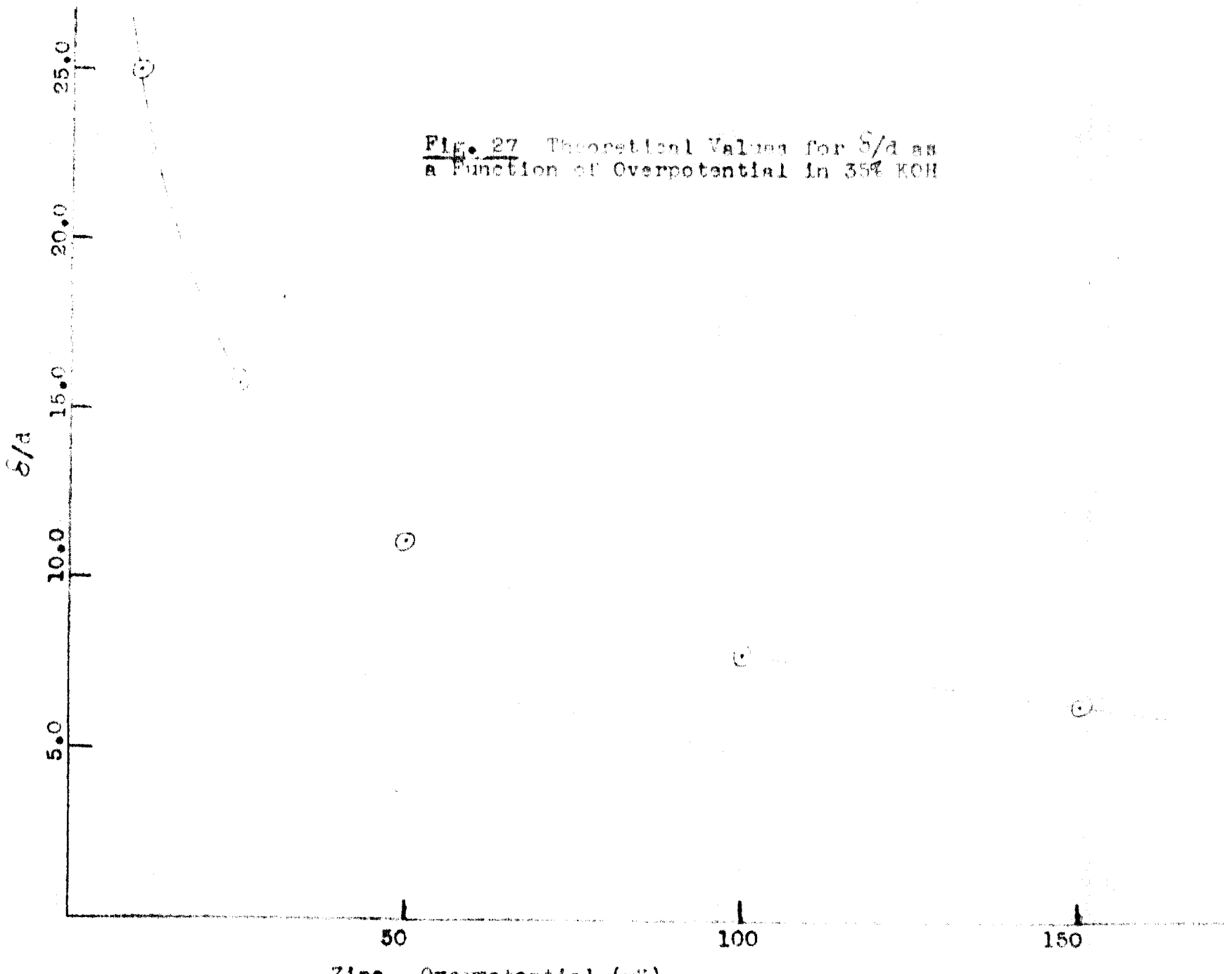

Fig. 27 Theoretical Values for δ/d as a Function of Overpotential in 35% KOH